

AFRL-VA-WP-TR-2003-3003

**CORROSION-INDUCED FATIGUE
MEASUREMENTS ON 2024 AND 7075
ALUMINUM USING PHOTON-
INDUCED POSITRON
ANNIHILATION (PIPA)**



D. W. Akers

**Positron Systems, Inc.
6151 N. Discovery Way
Boise, ID 83713**

DECEMBER 2002

Final Report for 01 April 2002 – 01 November 2002

THIS IS A SMALL BUSINESS INNOVATION RESEARCH (SBIR) PHASE 1 REPORT

Approved for public release; distribution is unlimited.

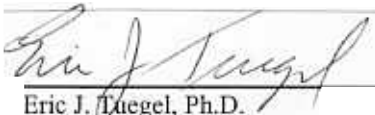
**AIR VEHICLES DIRECTORATE
AIR FORCE MATERIEL COMMAND
AIR FORCE RESEARCH LABORATORY
WRIGHT-PATTERSON AIR FORCE BASE, OH 45433-7542**

NOTICE


USING GOVERNMENT DRAWINGS, SPECIFICATIONS, OR OTHER DATA INCLUDED IN THIS DOCUMENT FOR ANY PURPOSE OTHER THAN GOVERNMENT PROCUREMENT DOES NOT IN ANY WAY OBLIGATE THE US GOVERNMENT. THE FACT THAT THE GOVERNMENT FORMULATED OR SUPPLIED THE DRAWINGS, SPECIFICATIONS, OR OTHER DATA DOES NOT LICENSE THE HOLDER OR ANY OTHER PERSON OR CORPORATION; OR CONVEY ANY RIGHTS OR PERMISSION TO MANUFACTURE, USE, OR SELL ANY PATENTED INVENTION THAT MAY RELATE TO THEM.

THIS REPORT HAS BEEN REVIEWED BY THE OFFICE OF PUBLIC AFFAIRS (ASC/PA) AND IS RELEASABLE TO THE NATIONAL TECHNICAL INFORMATION SERVICE (NTIS). AT NTIS, IT WILL BE AVAILABLE TO THE GENERAL PUBLIC, INCLUDING FOREIGN NATIONS.


THIS TECHNICAL REPORT HAS BEEN REVIEWED AND IS APPROVED FOR PUBLICATION.



Eric J. Tiegel, Ph.D.
Engineer
Aircraft Structural Integrity



James W. Rogers, Major, USAF
Chief
Analytical Structural Mechanics Branch



Jeffrey S. Turcotte, Lt. Col., USAF
Chief
Structures Division

This report is published in the interest of scientific and technical information exchange and does not constitute approval or disapproval of its ideas or findings.

Do not return copies of this report unless contractual obligations or notice on a specific document requires its return.

| REPORT DOCUMENTATION PAGE | | | | <i>Form Approved</i> <i>OMB No. 0704-0188</i> | |
|---|------------------------------------|-------------------------------------|---|---|---|
| <small>The public reporting burden for this collection of information is estimated to average 1 hour per response, including the time for reviewing instructions, searching existing data sources, gathering and maintaining the data needed, and completing and reviewing the collection of information. Send comments regarding this burden estimate or any other aspect of this collection of information, including suggestions for reducing this burden, to Department of Defense, Washington Headquarters Services, Directorate for Information Operations and Reports (0704-0188), 1215 Jefferson Davis Highway, Suite 1204, Arlington, VA 22202-4302. Respondents should be aware that notwithstanding any other provision of law, no person shall be subject to any penalty for failing to comply with a collection of information if it does not display a currently valid OMB control number. PLEASE DO NOT RETURN YOUR FORM TO THE ABOVE ADDRESS.</small> | | | | | |
| 1. REPORT DATE (DD-MM-YY) December 2002 | | 2. REPORT TYPE Final | | 3. DATES COVERED (From - To) 04/01/2002 – 11/01/2002 | |
| 4. TITLE AND SUBTITLE CORROSION-INDUCED FATIGUE MEASUREMENTS ON 2024 AND 7075 ALUMINUM USING PHOTON-INDUCED POSITRON ANNIHILATION (PIPA) | | | | 5a. CONTRACT NUMBER F33615-02-M-3203 | |
| | | | | 5b. GRANT NUMBER | |
| | | | | 5c. PROGRAM ELEMENT NUMBER 65502F | |
| 6. AUTHOR(S) D. W. Akers | | | | 5d. PROJECT NUMBER 3005 | |
| | | | | 5e. TASK NUMBER 42 | |
| | | | | 5f. WORK UNIT NUMBER 2J | |
| 7. PERFORMING ORGANIZATION NAME(S) AND ADDRESS(ES) Positron Systems, Inc. 6151 N. Discovery Way Boise, ID 83713 | | | | 8. PERFORMING ORGANIZATION REPORT NUMBER | |
| 9. SPONSORING/MONITORING AGENCY NAME(S) AND ADDRESS(ES) Air Vehicles Directorate Air Force Research Laboratory Air Force Materiel Command Wright-Patterson AFB, OH 45433-7542 | | | | 10. SPONSORING/MONITORING AGENCY ACRONYM(S) AFRL/VASM | |
| | | | | 11. SPONSORING/MONITORING AGENCY REPORT NUMBER(S) AFRL-VA-WP-TR-2003-3003 | |
| 12. DISTRIBUTION/AVAILABILITY STATEMENT Approved for public release; distribution is unlimited. | | | | | |
| 13. SUPPLEMENTARY NOTES THIS IS A SMALL BUSINESS INNOVATION RESEARCH (SBIR) PHASE 1 REPORT. Report contains color. | | | | | |
| 14. ABSTRACT Corrosion-related fatigue damage in aerospace platforms is a significant problem for military aircraft, which, in many cases, are over 20 years old and have projected lifetimes up to 40 years. Specific problems include multilayer corrosion damage in aircraft lap slices that result in cracking at fastener holes and rapid crack growth. A new nondestructive examination technique, photon-induced positron annihilation (PIPA), has demonstrated the capability to detect and quantify various types of atomic lattice structure damage, including fatigue, creep, and other mechanisms. The purpose of this project is to evaluate the PIPA technology to assess the effects of relatively low levels of corrosion on early fatigue damage, and to provide an approach for incorporating data of this type into developing confidence levels for CBM reliability models. Specimens of 2024-T3 and 7075-T6 aluminum were subjected to salt spray corrosion for periods up to 96 hours and then subjected to fatigue testing to determine the effects of the corrosion on the fatigue response for these types of aluminum, which have different corrosion characteristics. PIPA results from this study indicate that corrosion-related fatigue damage is detectable at relatively low fatigue levels (<10% of failure) and that damage to the inside surface of the aluminum specimens is also detectable. | | | | | |
| 15. SUBJECT TERMS corrosion, fatigue, damage accumulation, aluminum alloys, positron annihilation | | | | | |
| 16. SECURITY CLASSIFICATION OF: | | | 17. LIMITATION OF ABSTRACT: SAR | 18. NUMBER OF PAGES 48 | 19a. NAME OF RESPONSIBLE PERSON (Monitor) Eric Tuegel 19b. TELEPHONE NUMBER (Include Area Code) (937) 904-6772 |
| a. REPORT Unclassified | b. ABSTRACT Unclassified | c. THIS PAGE Unclassified | | | |

TABLE OF CONTENTS

| <u>Section</u> | <u>Page</u> |
|---|-------------|
| LIST OF FIGURES..... | iv |
| LIST OF TABLES..... | v |
| EXECUTIVE SUMMARY | 1 |
| 1.0 INTRODUCTION | 4 |
| 2.0 RECENT CORROSION RELATED FATIGUE RESEARCH | 6 |
| 3.0 TEST PLAN AND 2024 AND 7075 AL SPECIFICATIONS | 8 |
| 3.1 2024-T3 Al and 7075-T6 Al Corrosion and Fatigue Test Plan | 8 |
| 3.2 2024 and 7075 Aluminum Sample Specifications..... | 8 |
| 4.0 CORROSION AND FATIGUE TEST RESULTS | 11 |
| 5.0 PIPA MEASUREMENT RESULTS AND ANALYSIS | 15 |
| 5.1 Fatigue Damage Detections in Aluminum Alloys using PIPA | 15 |
| 5.2 PIPA 2024 and 7075 Al Corrosion-Induced Fatigue Damage | 16 |
| 5.3 2024 and 7075 PIPA Response to Corrosion-Induced Fatigue Damage | 18 |
| 6.0 CONCLUSIONS | 26 |
| 7.0 PHASE II WORK PLAN | 28 |
| 8.0 REFERENCES | 29 |
| APPENDIX A | 31 |
| LIST OF ACRONYMS | 37 |

LIST OF FIGURES

| <u>Figure</u> | <u>Page</u> |
|---|-------------|
| 1. Representative Test Specimen | 8 |
| 2. PIPA Fatigue Response | 16 |
| 3. PIPA Analysis Area | 17 |
| 4. PIPA Response to Corrosion for 7075 Samples | 20 |
| 5. 2024 Fatigue Damage at 6000 Cycles | 22 |
| 6. 7075 Fatigue Damage at 6000 Cycles | 22 |
| 7. 2024 Damage after 11,000 Cycles | 25 |
| 8. 7075 Damage after 6,000 and 11,000 Cycles | 25 |
| A1. Photon Induced Positron Annihilation Process | 32 |
| A2. Defect Characterization | 33 |
| A3. Positron Lifecycle | 33 |
| A4. Positron Annihilation Measurement Techniques | 35 |
| A5. Doppler Broadening Analysis for the S Parameter | 36 |

LIST OF TABLES

| <u>Table</u> | <u>Page</u> |
|---|-------------|
| 1. 2024 and 7075 Aluminum Corrosion and Fatigue Test Program | 9 |
| 2. 2024 and 7075 Aluminum Specimen Sample Preparation | 10 |
| 3. 2024 and 7075 Original Sample Dimensions | 10 |
| 4. 2024 and 7075 Specimen Dimensions Following Corrosion Testing | 12 |
| 5. 2024 and 7075 Specimen Dimensions Following First Fatigue Cycle | 12 |
| 6. 2024 and 7075 Specimen Dimensions Following Second Fatigue Cycle | 13 |
| 7. 2024 and 7075 Specimen Dimension Change Following First Fatigue Cycle | 13 |
| 8. 2024 and 7075 Specimen Dimension Change Following Second Fatigue Cycle | 14 |
| 9. Reproducible Measurements of 2024 Blank Aluminum Specimens | 18 |
| 10. 2024 PIPA Corrosion Response | 19 |
| 11. 7075 PIPA Corrosion Response | 19 |
| 12. 2024 Aluminum Exposed to Corrosion and 6000 Fatigue Cycles | 21 |
| 13. 7075 Aluminum Exposed to Corrosion and 6000 Fatigue Cycles | 21 |
| 14. 2024 Aluminum Exposed to Corrosion and up to 12,000 Fatigue Cycles | 24 |
| 15. 7075 Aluminum Exposed to Corrosion and up to 12,000 Fatigue Cycles..... | 24 |

EXECUTIVE SUMMARY

Condition-based maintenance (CBM) is the current maintenance approach utilized by the Air Force to assess maintenance requirements for specific components and aircraft. Specific issues identified with implementing CBM include defining fatigue damage algorithms that can: (1) assess corrosion fatigue damage accurately; (2) predict how the damage will grow; and (3) provide a reliability measure for (1) and (2). However, no reliability measure (or estimate of the confidence in the results) is constructed in this model. The reliability measure should include the confidence or uncertainty associated with the damage detection and the confidence in the prediction of damage growth and remaining life.

Although there are many potential problems associated with corrosion-induced fatigue, an example of a key damage problem is the cracking and failure at lap splice locations in several of the Air Force's tanker and transport aircraft. Corrosion at various subsurface locations results in crack initiation and growth from fastener-hole locations. It has been shown that the small cracks can grow rapidly to large cracks. Detection of corrosion damage and fatigue growth at the buried lap splice locations is a principal problem that has not been well addressed at this point.

The development of fatigue damage algorithms for appropriate reliability measures (or uncertainties) that can be implemented in CBM models requires methods that allow fatigue damage to be detected and accurately quantified. In addition, the method used should be suitable for quantifying the effects of corrosion directly or the effect of the corrosion on fatigue damage and remaining life. The recently developed PIPA technology has demonstrated a robust capability for detecting lattice structure damage in materials at any point during the life of a material or component. The purpose of this project is to evaluate the PIPA technology to assess the effects of relatively low levels of corrosion on early fatigue damage, and to provide an approach for incorporating data of this type into developing confidence levels for CBM reliability models.

Prior studies using PIPA indicate this technique is sensitive to fatigue damage and that this type of failure mechanism is detectable and quantifiable by PIPA. Recent work demonstrating PIPA's ability to detect fatigue damage is presented in this paper. However, in previous studies, the specimens prepared were more similar to actual lap splices in that holes had been placed as stress concentrators. The presence of the stress concentrators improves the sensitivity of the PIPA technique to the subtle microstructural changes that appear to be associated with high cycle fatigue damage. However, in this study the specimens of 2024-T3 and 7075-T6 aluminum prepared were thin (.080 in. sheets) with no stress concentrator holes. Consequently the sensitivity is less than would be expected for samples with stress concentrators.

The aluminum alloys used in this study were chosen because they are common alloys and because the 7075-T6 alloy is considered particularly susceptible to corrosion and stress corrosion cracking (SCC). Therefore, samples with relatively good and poor corrosion response characteristics are being tested. The samples prepared for this program were standard dog bone specimens with a length of 6 inches and a gauge section length of 1.0 in. (width 0.5 in.) Corrosion testing was performed for 24 hours, 48 hours (24 hours per side, to simulate buried corrosion in a lap splice) and 96 hours. The fatigue test procedure used a fatigue stress of 129

MPa, which is low for aircraft high cycle fatigue damage; however, untreated samples failed in the range between about 25,000 and 30,000 cycles. This failure point is very low when compared to the literature (nominally 5-10%). Some variations in the sample preparation (bar stock specimens) and processing parameters during the fatigue testing may have contributed to these early cycle failures. It should be noted that a complete set of specimens was prepared and tested initially and it was later determined that the corrosion testing had been performed improperly (over-corroded). Polished round or improved bar specimens and better quality control are proposed for follow on work to minimize sample damage during preparation and optimize the testing.

As noted above, the purpose of this project was to provide suitable data that can be used in the development of fatigue models, the uncertainties associated with these models, and to provide a method for better determining remaining life based on the PIPA response. The specific objectives were to determine:

- Can PIPA be used to detect the effect of corrosion on the lattice structure of the material and can buried corrosion (multi-layer) be detected?
- Can the effect of the corrosion on the fatigue response be detected?
- Can the effect of the corrosion be differentiated between an alloy that is highly susceptible to fatigue from one that is not?
- Does the PIPA data provide sufficient information that could ultimately be used to develop reliability models?

PIPA measurements were performed on the 2024-T3 and 7075-T6 specimens following exposure to a corrosive salt spray solution for 24 hrs, 48 hrs (24 hrs per side) and 96 hours. This was done as a test to assess the average response from the material, as it was not expected that direct thin layer (10-20 micron pitting) corrosion would be directly detectable. However, the results indicated that the corrosion effect is distinctly detectable as compared to the virgin material specimen. The PIPA measurements detected a significant reduction in the S parameter between the blank material and the corroded material, indicating some effect on the material. Currently, more research would be required to understand why this response occurred.

Review of the literature provides little current information that would help to understand this effect although some follow on measurements to assess the corrosion penetration into the two alloys and SEM measurements would provide additional data for comparison purposes. Also, the results show some scatter, largely because as is true in operational environments, corrosion is not evenly deposited on component surfaces. Further, the corrosion is not evenly distributed on the aluminum and because the PIPA examination area used for these measurements was about .20 in², this could result in some scatter. Because of this variability, further work will be performed using a larger measurement area (1.0 in.²) to reduce the variability and provide average response data. In addition, we are currently planning some pit depth measurements to obtain a better measure of the actual average pit depths on these specimens.

The next objective was to assess the effects of fatigue testing on the material. In this case, the samples were cycled to two levels, 6000, and 11000 cycles. Based on the literature these would be expected to be relatively small fractions of the fatigue life at 129 MPa. Results of the fatigue

testing for the two types of aluminum resulted in an increase in the PIPA response for the corroded 7075 material (indicating an increase in fatigue damage) and little change in the response for the 2024 material. Although the uncertainties are relatively large at this low level of damage and due to possible variations in the corrosion levels from sample to sample, the trend data are clear and, in some cases, statistically significant. The likely mechanism that appears to have resulted in the growth of fatigue damage in the 7075 material is increased pitting from corrosion that helped function as a stress concentrator in the material, thereby increasing the response for the 7075-T6 material relative to the 2024-T3. Consequently, the data suggest that PIPA can detect corrosion induced fatigue changes and differentiate the response of more to less highly corroded and fatigued materials. Further work is needed to optimize the fatigue response with work done on specimens with a more even distribution of corrosion and with larger PIPA examination areas to produce a better average response.

Concerning the use of the PIPA data for the development of reliability algorithms to define uncertainties associated with corrosion-induced fatigue buildup, we believe further work is required to 1) optimize the sample preparation and testing (including fastener holes in some specimens), 2) perform measurements using the improved PIPA measurement and analysis process that has been developed since these measurements were performed, 3) perform SEM and X-ray diffraction measurements for comparison with the PIPA results, 4) obtain sufficient data at higher corrosion and fatigue levels to develop appropriate damage curves, 5) perform measurements on actual aircraft components (e.g., lap splices) with operational corrosion damage, and 6) develop a suitable database so that the uncertainties can be better defined for use in the development of a small, laboratory based Neutron Induced Positron Annihilation (NIPA) unit.

Follow on work in a Phase Two effort would be first to address the issues above that would allow the uncertainties identified in this study to be reduced, and to begin development of suitable data that could be used in the development of uncertainties for fatigue models for components subjected to this type of damage. Comparison data should be obtained for aircraft components at various stages of life through failure with damage levels that would be validated through microstructural measurements. As compared to other measurement technologies that we have surveyed, PIPA has potential to be able to provide useful information on corrosion-induced fatigue that is not available through other techniques; however further work will be required to better understand the mechanisms and failure behavior involved, and to provide a suitable field use capability for measuring damage and quantifying remaining life in current aircraft structures.

1.0 INTRODUCTION

Corrosion-related fatigue damage resulting in the failure of aluminum aircraft structures has been shown to be a critical issue for the U. S. military and has been shown to significantly increase maintenance requirements and reduce the operational life of many components. This is a serious problem for currently operated military aircraft, as many are more than 20 years old with projected lifetimes of up to 40 years. Significant effort has gone into the development of models to predict crack growth and potential failure modes [1,2,3]. However, these models have been severely limited because of the lack of good measurement data on the dislocation phenomena that result in crack formation, propagation and failure, and ways to assess the progression of damage in existing aircraft.

Although there are many potential problems associated with corrosion-induced fatigue an example of a key damage problem is the cracking and failure at lap splice locations in large military transport and tanker aircraft [4,5]. In this case, the problem is the presence of corrosion at various subsurface locations that results in crack initiation and rapid growth from fastener hole locations. It has been shown that this damage can grow rapidly and result in large cracks. Detection of corrosion damage and fatigue growth at the buried lap splice locations has not been accomplished and there is limited data that is usable for the development of models needed to predict failure or even the likelihood of failure prior to the next inspection. Both the feasibility of using the PIPA technology to detect damage of this type before crack initiation and assessing its potential capability to develop data that can be used to predict the likelihood of failure and/or the probability of reaching the next inspection period before failure are the end goals of this research effort.

The purpose of this research initiative is to demonstrate the capability of the PIPA technology to detect and quantify corrosion-induced fatigue damage and to show that the process provides data that can be used for developing and improving models to predict the effects of corrosion on fatigue damage, potential failure modes, and crack growth behavior. In more practical terms, it would be used to assess issues similar to those for aircraft structural joints where both multi-layer detection and the ability to predict when cracking may begin are critical. Specific objectives include:

- Can PIPA be used to detect the effect of corrosion on the lattice structure of the material and can buried corrosion be detected?
- Can the effect of the corrosion on the fatigue response be detected?
- Can the effect of the corrosion be differentiated between an alloy that is highly susceptible to fatigue from one that is not?
- Does the PIPA data provide sufficient information that could ultimately be used to develop reliability models?

The elements of this study include performing corrosion testing using a salt spray on 2024-T3 and 7075-T6 aluminum to various corrosion levels, and fatigue testing of the samples to several fatigue levels short of failure with PIPA testing after each stage of fatigue or corrosion testing. Two sets of test specimens were prepared and tested for this using the ASTM G85 modified salt/spray fog corrosion test. However, for the first series of tests and measurements, it was

determined that the test procedure was not strictly followed at the material testing laboratory, which produced results that were generally unusable (samples were over-corroded). The second series of corrosion tests were performed using more acceptable procedures and processes. Unfortunately, it was not determined that the first set of measurements was unacceptable until all PIPA measurements were complete. Consequently, the first series data were excluded from this report.

The following sections present:

- A summary of recent research on fatigue damage effects on aluminum;
- The test plan and 2024 and 7075 sample preparation and test data;
- Fatigue and corrosion test results including dimensional change data;
- Sample examination results and analysis, including the assessment of both isolated corrosion and corrosion/fatigue damage;
- Application of current results to possible model development;
- Follow-on research needed to complete the development of the PIPA technique for use in both the development of reliability algorithms and in periodic testing of aircraft structures to determine the probability of failure prior to the next inspection series.

2.0 RECENT CORROSION RELATED FATIGUE RESEARCH

Recent research on the effects of corrosion on aluminum and fatigue failure provides information on the possible mechanisms resulting in damage, penetration depths and the results of other corrosion test studies for comparison with the results of the PIPA corrosion/fatigue measurements performed as part of this study. Initial requirements for this study are based on corrosion-induced fatigue damage studies that are based on aircraft corrosion/fatigue issues. A key problem as noted above is the presence of multi-layer corrosion in aircraft 2024 aluminum structural joints; including butt and lap splice joints. Fatigue damage has been shown to be enhanced by the presence of corrosion resulting in the rapid production of large cracks at some locations in the structural joints [6]. These research results are presented to aid in the interpretation of the PIPA results obtained as part of this study.

Representative studies of the effects of corrosion on the fatigue behavior of aluminum indicate that corrosion can result in the reduction of the fatigue strength of 7075-T6 aluminum alloys by up to 40% [7,8]. In contrast, other studies suggest that the 2024-T3 alloy is less susceptible to corrosion. These studies also show that the pit growth is typically aligned with the rolling direction and that the damage visibly occurred in patches on the surface of the material being exposed to the corrosion. Pitting depth also appears to have increased relative linearly from average depths of about 9 micron at 24 hours to 8 to 12 micron at 48 hours, and to about 14 micron at 96 hours for the 7075 material. It should be noted that the average length and width of the corrosion zones increased rapidly after 24 hours and were nearly constant at 48 and 96 hours, suggesting that after 24 hours increased damage was due to increases in pit depth rather than increased surface attack.

For periods greater than 96 hours the corrosion resulted in increased pit depths and lower numbers of pits at longer exposure periods with depths ranging from about 36 micron to 72 micron at 1500 hours. Other studies would suggest that this is probably a higher level of corrosion relative to other alloys of aluminum such as 2024, which are expected to be less susceptible to corrosion attack.

As part of the study noted above, the previously corroded 7075 aluminum specimens were subjected to constant amplitude fatigue testing at various stress levels up to 414 MPa. This study and others indicated that the pre-existing corrosion can result in crack initiation at levels as low as 15% of the total life of non corroded specimens (i.e., for 2024 aluminum) [9]. This study showed a reduction in the fatigue lives of 7075-T6 by factors of 6-8. Typically, this study was performed at stress levels ranging from 300-450 MPa whereas the work performed in this research project was done at a considerably lower stress level, 129 MPa.

Other studies of changes in the tensile and energy properties of various types of aluminum have indicated major changes related to the presence of corrosion. Changes in the elongation and yield stress of the aluminum materials have been indicated [10]. In addition, other effects have been identified including the load frequency that can affect corrosion-induced fatigue damage initiation and buildup [11]. Chen indicated that for frequencies under 5 Hz (our study was performed at 2 Hz) that the fatigue threshold criterion (ΔK_{tr} - MPa \sqrt{m}) increased with decreasing frequency. For 2024 Al at 288 MPa at 1 Hz, ΔK_{tr} was at 3.29 MPa \sqrt{m} . Consequently, they

suggested that there is a transition from pitting to fatigue crack growth that occurs at the fatigue threshold stress intensity factor (ΔK_{tr}) and there is rate competition between the pit growth and corrosion crack growth. This suggests that there may be a transition point in the response for some materials that may be detectable.

Consequently, the relevance of these data to our study suggests that there are significant effects from corrosion on the fatigue life of aluminum alloys being tested. Principal observations are that the 7075-T6 Al is likely to be less corrosion resistant than the 2024-T3 Al with corresponding changes in the material properties induced by the corrosion. There also may be a transition point from corrosion-induced damage to fatigue-induced damage when the fatigue threshold intensity factor is reached. Further, because of the sensitivity of the PIPA technique other mechanistic differences may be detectable.

3.0 TEST PLAN AND 2024 AND 7075 AL SPECIFICATIONS

The test plan and the specifications for the 2024 and 7075 aluminum specimens used for the PIPA testing program along with the designation and initial dimensions of the samples tested are discussed below. Two series of specimens were tested; however it was determined that during the first series of corrosion tests that the specimens were turned over after some series of corrosion tests, followed by over-corroding. Consequently the first series of data are not being used for this project.

3.1 2024-T3 Al and 7075-T6 Al Corrosion and Fatigue Test Plan

The test plan for this project was defined based on specifications identified by the AFRL project manager. In this case, it was decided to prepare a sufficient number of specimens of 2024-T3 and 7075-T6 series aluminum alloys such that 3 specimens were present for each condition measured. This resulted in a total of 16 specimens prepared for each alloy with blanks. The test plan for this program and each sample are defined in Table 1.

The corrosion testing was performed using a Q Fog Environmental Chamber and the Fatigue testing was performed with an Instron Load Frame (Model 8862). The composition of the corrosion test solution was the salt solution formula identified in the Annex from the ASTM G85.

3.2 2024 and 7075 Aluminum Sample Specifications

The basic sample specifications that were identified for this project are listed in Table 2. The specimens used were bare aluminum, which is more susceptible to corrosion than that with a surface treatment used for commercial applications. Figure 1 shows an example specimen.



Figure 1. Representative Test Specimen

Table 1. 2024 and 7075 Aluminum Corrosion and Fatigue Test Program

| Requirement | | | Number of Specimens | | |
|-----------------------------|---------|--------------|---------------------|--------|---|
| Sample preparation protocol | | | 16 (each alloy) | | ASTM E606 |
| Corrosion test protocol | | | | | ASTM G85 – salt spray test |
| Fatigue test requirements | | | | | G85 cyclic A2 procedure |
| Fatigue frequency | | | 2 Hz | | |
| Mean load/amplitude | | | 750/650 | | |
| Stress | | | 18750/16250 PSI | | 129/125 MPa |
| ID | Alloy | Exposure(hr) | Cycles | Cycles | Comments |
| 2-17 | 2024 T3 | 0 | 6000 | 5000 | |
| 2-18 | 2024 T3 | 0 | 6000 | 5000 | |
| 2-19 | 2024 T3 | 0 | 6000 | 5000 | |
| 2-20 | 2024 T3 | 24 | 6000 | 5000 | |
| 2-21 | 2024 T3 | 24 | 6000 | 5000 | |
| 2-22 | 2024 T3 | 24 | 6000 | 5000 | |
| 2-23 | 2024 T3 | 24/24 | 6000 | 5000 | Samples exposed to 24 hours on each side of the three specimens |
| 2-24 | 2024 T3 | 24/24 | 6000 | 5000 | |
| 2-25 | 2024 T3 | 24/24 | 6000 | 5000 | |
| 2-26 | 2024 T3 | 96 | 6000 | 5000 | Noted |
| 2-27 | 2024 T3 | 96 | 6000 | 5000 | |
| 2-28 | 2024 T3 | 96 | 6000 | 5000 | |
| 2-29 | 2024 T3 | 96 | 13225 | na | Normal cycles to failure |
| 2-30 | 2024 T3 | blk | | | |
| 2-31 | 2024 T3 | blk | | | |
| 2-32 | 2024 T3 | blk | | | |
| ID | Alloy | Exposure(hr) | Cycles | Cycles | Comments |
| 7-17 | 7075 T6 | 0 | 7000 | 5000 | 6000 plus additional 1000 cycles |
| 7-18 | 7075 T6 | 0 | 7000 | 5000 | |
| 7-19 | 7075 T6 | 0 | 7000 | 5000 | |
| 7-20 | 7075 T6 | 24 | 6946 | na | Failed early, lowered target back to 6000 cycles |
| 7-21 | 7075 T6 | 24 | 6000 | 5000 | |
| 7-22 | 7075 T6 | 24 | 6000 | 5000 | |
| 7-23 | 7075 T6 | 24/24 | 6000 | 1297 | Failed early |
| 7-24 | 7075 T6 | 24/24 | 6000 | 2899 | Failed early |
| 7-25 | 7075 T6 | 24/24 | 6000 | 2562 | Failed early |
| 7-26 | 7075 T6 | 96 | 6000 | 5000 | |
| 7-27 | 7075 T6 | 96 | 6000 | 3400 | Failed early |
| 7-28 | 7075 T6 | 96 | 6000 | 3060 | Failed early |
| 7-29 | 7075 T6 | 96 | 14350 | na | Normal cycles to failure |
| 7-30 | 7075 T6 | blk | 29100 | na | Normal cycles to failure |
| 7-31 | 7075 T6 | blk | | | |
| 7-32 | 7075 T6 | blk | | | |

Table 2. 2024 and 7075 Aluminum Specimen Sample Preparation

| | |
|------------------------------|-------------------------|
| 2024-T3 and 7075-T6 Aluminum | Uncoated bare aluminum |
| Length | 6 in. |
| Gage length | 1 in. |
| Width in the gage | 0.5 in. |
| Thickness | 0.080 in. |
| Edges of specimens | Coated with nail polish |

Initial dimensions for each specimen tested are listed in Table 3. As indicated there are small variations in both the length and thickness of each sample; however, the specimens are not significantly different with most deviations occurring at less than 0.02 in.

Table 3. 2024 and 7075 Original Specimen Dimensions

| Specimen ID | Length (in) | Gage Width (in) | Gage Thickness (in) | Overall Length (in) | Gage Width (in) | Gage Thickness (in) |
|-----------------------|---------------|-----------------|---------------------|-----------------------|-----------------|---------------------|
| 2024-T3 Series | | | | 7075-T6 Series | | |
| 2-17 | 6.0325 | 0.5040 | 0.0815 | 7-17 | 6.0290 | 0.5105 |
| 2-18 | 6.0130 | 0.5055 | 0.0815 | 7-18 | 6.0155 | 0.5050 |
| 2-19 | 5.9695 | 0.5060 | 0.0820 | 7-19 | 6.0315 | 0.5085 |
| 2-20 | 6.0250 | 0.5050 | 0.0825 | 7-20 | 6.0300 | 0.5040 |
| 2-21 | 6.0210 | 0.5060 | 0.0815 | 7-21 | 6.0340 | 0.5065 |
| 2-22 | 6.0175 | 0.5020 | 0.0815 | 7-22 | 6.0170 | 0.5090 |
| 2-23 | 5.9535 | 0.5040 | 0.0820 | 7-23 | 5.9955 | 0.5085 |
| 2-24 | 6.0325 | 0.5020 | 0.0815 | 7-24 | 5.9940 | 0.5090 |
| 2-25 | 6.0100 | 0.5040 | 0.0815 | 7-25 | 6.0105 | 0.5100 |
| 2-26 | 6.0280 | 0.5060 | 0.0815 | 7-26 | 6.0350 | 0.5120 |
| 2-27 | 5.9685 | 0.5020 | 0.0815 | 7-27 | 6.0335 | 0.5105 |
| 2-28 | 6.0290 | 0.5050 | 0.0815 | 7-28 | 5.9965 | 0.5050 |
| 2-29 | Not Available | | | 7-29 | Not Available | |
| 2-30 - Blank | 6.0230 | 0.5045 | 0.0815 | 7-30 | Not Available | |
| 2-31 - Blank | 5.9610 | 0.5055 | 0.0815 | 7-31 | 5.9945 | 0.5090 |
| 2-32 - Blank | 6.0250 | 0.5035 | 0.0810 | 7-32 | 6.0265 | 0.5065 |

4.0 CORROSION AND FATIGUE TEST RESULTS

This section presents the results of the corrosion and fatigue testing that was performed on the specimens identified in the previous section. As noted in the test plan the specimens were corrosion tested for periods of 24 and 96 hours, and one set of specimens was corroded for 24 hours on each side of the specimen to assess the effects of multilayer corrosion.

Table 4 lists the dimensional information for these specimens following corrosion testing and Tables 5 and 6 list the dimensions after the first and second fatigue cycles. Tables 7 and 8 show the relative change in the specimen dimensions for each sample. Specimens where there was a significant elongation due to the fatigue testing have been identified in the tables.

Examination of Tables 7 and 8 indicates that only a few samples exhibited any elongation and that the ones that did were small (~0.01 in.). Consequently, for the fatigue testing done there appeared to be little elongation prior to failure. There were concerns for this second set of samples that there might be a failure location that was induced when the samples were cut at the edge of the samples' gage sections as most failures occurred away from the center and at the edge of the gage section.

Table 4. 2024 and 7075 Specimen Dimensions Following Corrosion Testing

| Specimen ID | Length (in) | Gage Width (in) | Gage Thickness (in) | | Overall Length (in) | Gage Width (in) | Gage Thickness (in) |
|-----------------------|---------------|-----------------|---------------------|-----------------------|---------------------|-----------------|---------------------|
| 2024-T3 Series | | | | 7075-T6 Series | | | |
| 2-17 | 6.0325 | 0.5040 | 0.0815 | 7-17 | 6.0290 | 0.5105 | 0.0800 |
| 2-18 | 6.0130 | 0.5055 | 0.0815 | 7-18 | 6.0155 | 0.5050 | 0.0805 |
| 2-19 | 5.9695 | 0.5060 | 0.0820 | 7-19 | 6.0315 | 0.5085 | 0.0805 |
| 2-20 | 6.0250 | 0.5050 | 0.0825 | 7-20 | 6.0300 | 0.5040 | 0.0805 |
| 2-21 | 6.0210 | 0.5060 | 0.0815 | 7-21 | 6.0340 | 0.5065 | 0.0805 |
| 2-22 | 6.0175 | 0.5020 | 0.0815 | 7-22 | 6.0170 | 0.5090 | 0.0805 |
| 2-23 | 5.9535 | 0.5040 | 0.0820 | 7-23 | 5.9955 | 0.5085 | 0.0805 |
| 2-24 | 6.0325 | 0.5020 | 0.0815 | 7-24 | 5.9940 | 0.5090 | 0.0805 |
| 2-25 | 6.0100 | 0.5040 | 0.0815 | 7-25 | 6.0105 | 0.5100 | 0.0805 |
| 2-26 | 6.0280 | 0.5060 | 0.0815 | 7-26 | 6.0350 | 0.5120 | 0.0805 |
| 2-27 | 5.9685 | 0.5020 | 0.0815 | 7-27 | 6.0335 | 0.5105 | 0.0805 |
| 2-28 | 6.0290 | 0.5050 | 0.0815 | 7-28 | 5.9965 | 0.5050 | 0.0805 |
| 2-29 | Not Available | | | 7-29 | Not Available | | |
| 2-30 - Blank | 6.0230 | 0.5045 | 0.0815 | 7-30 | Not Available | | |
| 2-31 - Blank | 5.9610 | 0.5055 | 0.0815 | 7-31 | 5.9945 | 0.5090 | 0.0805 |
| 2-32 - Blank | 6.0250 | 0.5035 | 0.0810 | 7-32 | 6.0265 | 0.5065 | 0.0800 |

Table 5. 2024 and 7075 Specimen Dimensions Following First Fatigue Cycle

| Specimen ID ^a | Overall Length | Gage Width | Gage Thickness | Specimen ID | Overall Length | Gage Width | Gage Thickness |
|--------------------------|----------------|------------|----------------|-----------------------|----------------|------------|----------------|
| 2024-T3 Series | | | | 7075-T6 Series | | | |
| 2-17 | 6.0285 | 0.5035 | 0.0810 | 7-17 | 6.0270 | 0.5100 | 0.0800 |
| 2-18 | 6.0150 | 0.5050 | 0.0810 | 7-18 | 6.0160 | 0.5045 | 0.0800 |
| 2-19 | 5.9675 | 0.5060 | 0.0810 | 7-19 | 6.0320 | 0.5080 | 0.0800 |
| 2-20 | 6.0285 | 0.5045 | 0.0815 | 7-20 | Broken | | |
| 2-21 | 6.0250 | 0.5055 | 0.0815 | 7-21 | 6.0340 | 0.5065 | 0.0805 |
| 2-22 | 6.0160 | 0.5020 | 0.0810 | 7-22 | 6.0205 | 0.5090 | 0.0805 |
| 2-23 | 5.9650 | 0.5035 | 0.0815 | 7-23 | 5.9980 | 0.5085 | 0.0805 |
| 2-24 | 6.0245 | 0.5015 | 0.0815 | 7-24 | 5.9945 | 0.5090 | 0.0805 |
| 2-25 | 6.0110 | 0.5035 | 0.0815 | 7-25 | 6.0100 | 0.5100 | 0.0805 |
| 2-26 | 6.0280 | 0.5060 | 0.0815 | 7-26 | 6.0345 | 0.5110 | 0.0805 |
| 2-27 | 5.9715 | 0.5020 | 0.0815 | 7-27 | 6.0340 | 0.5095 | 0.0805 |
| 2-28 | 6.0250 | 0.5050 | 0.0820 | 7-28 | 5.9965 | 0.5045 | 0.0805 |

a. Blank specimens were not remeasured as no dimensional change would occur

Table 6. 2024 and 7075 Specimen Dimensions Following Second Fatigue Cycle

| Specimen ID | Overall Length | Gage Width | Gage Thickness | Specimen ID | Overall Length | Gage Width | Gage Thickness |
|-----------------------|----------------|------------|----------------|-----------------------|----------------|------------|----------------|
| 2024-T3 Series | | | | 7075-T6 Series | | | |
| 2-17 | 6.0290 | 0.5035 | 0.0810 | 7-17 | 6.0270 | 0.5100 | 0.0800 |
| 2-18 | 6.0150 | 0.5045 | 0.0810 | 7-18 | 6.0155 | 0.5045 | 0.0800 |
| 2-19 | 5.9615 | 0.5055 | 0.0810 | 7-19 | 6.0315 | 0.5080 | 0.0800 |
| 2-20 | 6.0270 | 0.5045 | 0.0810 | 7-20 | Broken | | |
| 2-21 | 6.0235 | 0.5055 | 0.0810 | 7-21 | 6.0340 | 0.5065 | 0.0805 |
| 2-22 | 6.0155 | 0.5015 | 0.0805 | 7-22 | 6.0205 | 0.5090 | 0.0805 |
| 2-23 | 5.9645 | 0.5035 | 0.0815 | 7-23 | Broken | | |
| 2-24 | 6.0250 | 0.5015 | 0.0810 | 7-24 | Broken | | |
| 2-25 | 6.0110 | 0.5035 | 0.0810 | 7-25 | Broken | | |
| 2-26 | 6.0280 | 0.5055 | 0.0810 | 7-26 | 6.0345 | 0.5110 | 0.0805 |
| 2-27 | 5.9725 | 0.5015 | 0.0810 | 7-27 | Broken | | |
| 2-28 | 6.0250 | 0.5045 | 0.0815 | 7-28 | Broken | | |
| 2-29 | Broken | | | 7-29 | Broken | | |
| 2-30 - Blank | 6.0225 | 0.5045 | 0.0810 | 7-30 | Broken | | |
| 2-31 - Blank | 5.9610 | 0.5055 | 0.0810 | 7-31 | 5.9945 | 0.5095 | 0.0805 |
| 2-32 - Blank | 6.0245 | 0.5035 | 0.0815 | 7-32 | 6.0265 | 0.5070 | 0.0805 |

Table 7. 2024 and 7075 Specimen Dimension Change Following First Fatigue Cycle

| Specimen ID | Change In | | | Specimen ID | Change In | | |
|-----------------------|----------------|-------------|----------------|-----------------------|----------------|------------|----------------|
| | Overall Length | Gage Width | Gage Thickness | | Overall Length | Gage Width | Gage Thickness |
| 2024-T3 Series | | | | 7075-T6 Series | | | |
| 2-17 | -0.0040 | -0.0005 | -0.0005 | 7-17 | -0.0020 | -0.0005 | 0.0000 |
| 2-18 | 0.0020 | -0.0005 | -0.0005 | 7-18 | 0.0005 | -0.0005 | -0.0005 |
| 2-19 | -0.0020 | 0.0000 | -0.0010 | 7-19 | 0.0005 | -0.0005 | -0.0005 |
| 2-20 | 0.0035 | -0.0005 | -0.0010 | 7-20 | Broken | | |
| 2-21 | 0.0040 | -0.0005 | 0.0000 | 7-21 | 0.0000 | 0.0000 | 0.0000 |
| 2-22 | -0.0015 | 0.0000 | -0.0005 | 7-22 | 0.0035 | 0.0000 | 0.0000 |
| 2-23 | 0.0115 | -0.0005 | -0.0005 | 7-23 | 0.0025 | 0.0000 | 0.0000 |
| 2-24 | -0.0080 | -0.0005 | 0.0000 | 7-24 | 0.0005 | 0.0000 | 0.0000 |
| 2-25 | 0.0010 | -0.0005 | 0.0000 | 7-25 | -0.0005 | 0.0000 | 0.0000 |
| 2-26 | 0.0000 | 0.0000 | 0.0000 | 7-26 | -0.0005 | -0.0010 | 0.0000 |
| 2-27 | 0.0030 | 0.0000 | 0.0000 | 7-27 | 0.0005 | -0.0010 | 0.0000 |
| 2-28 | -0.0040 | 0.0000 | 0.0005 | 7-28 | 0.0000 | -0.0005 | 0.0000 |
| | Average | | | | Average | | |
| | S.D | | | | S.D | | |
| | 0.0005 | -0.0003 | -0.0003 | | 0.0005 | -0.0004 | -0.0001 |
| | 0.004992988 | 0.000257464 | 0.00045 | | 0.00147402 | 0.00039312 | 0.000202 |

Table 8. 2024 and 7075 Specimen Dimension Change Following Second Fatigue Cycle

| Specimen ID | Change In | | | | Change In | | |
|-----------------------|----------------|-------------|----------------|-----------------------|----------------|------------|----------------|
| | Overall Length | Gage Width | Gage Thickness | | Overall Length | Gage Width | Gage Thickness |
| 2024-T3 Series | | | | 7075-T6 Series | | | |
| 2-17 | -0.0035 | -0.0005 | -0.0005 | 7-17 | -0.0020 | -0.0005 | 0.0000 |
| 2-18 | 0.0020 | -0.0010 | -0.0005 | 7-18 | 0.0000 | -0.0005 | -0.0005 |
| 2-19 | -0.0080 | -0.0005 | -0.0010 | 7-19 | 0.0000 | -0.0005 | -0.0005 |
| 2-20 | 0.0020 | -0.0005 | -0.0015 | 7-20 | Broken | | |
| 2-21 | 0.0025 | -0.0005 | -0.0005 | 7-21 | 0.0000 | 0.0000 | 0.0000 |
| 2-22 | -0.0020 | -0.0005 | -0.0010 | 7-22 | 0.0035 | 0.0000 | 0.0000 |
| 2-23 | 0.0110 | -0.0005 | -0.0005 | 7-23 | Broken | | |
| 2-24 | -0.0075 | -0.0005 | -0.0005 | 7-24 | Broken | | |
| 2-25 | 0.0010 | -0.0005 | -0.0005 | 7-25 | Broken | | |
| 2-26 | 0.0000 | -0.0005 | -0.0005 | 7-26 | -0.0005 | -0.0010 | 0.0000 |
| 2-27 | 0.0040 | -0.0005 | -0.0005 | 7-27 | Broken | | |
| 2-28 | -0.0040 | -0.0005 | 0.0000 | 7-28 | Broken | | |
| Average | -0.0002 | -0.0005 | -0.0006 | | 0.0002 | -0.0004 | -0.0002 |
| S.D. | 0.005259011 | 0.000144338 | 0.000377 | | 0.00180739 | 0.00037639 | 0.000258 |

5.0 PIPA MEASUREMENT RESULTS AND ANALYSIS

The objective of this section is to present the results of the PIPA measurements on specimens that have been subjected to fatigue damage, corrosion damage and combined corrosion-fatigue damage. Several initial studies have been performed on aluminum using surface positron techniques that discuss the sensitivity of the positron annihilation technique to changes in the material microstructure at the nano level. In addition, there are a number of general texts describing the basic physics of the positron annihilation measurement technique that provide significant information on the analysis methods used for the PIPA technique [12,13,14,15,16,17,18,19]. However, there is limited information on the PIPA measurement technique in the literature, consequently we have included a description of the PIPA technique and a description of the process in Appendix A. The following sections address the direct PIPA response to various levels of fatigue damage, the PIPA response to direct corrosion damage, and the corrosion-induced fatigue damage response from the samples in the current study.

5.1 Fatigue Damage Detection in Aluminum Alloys using PIPA

Several studies using the PIPA technique have been performed to assess fatigue damage in aluminum alloys. The results of one study where a lap splice joint was simulated with a hole in the center as a stress concentrator is shown. These data are being presented as they have some relevance to the detection of corrosion-induced fatigue damage in aircraft components. In this study, specimens of 7075 aluminum with a hole at the center of each specimen (to simulate a lap splice joint hole), and to act as a stress concentrator, were subjected to fatigue damage up to a failure point of about 345,000 cycles. Figure 2 shows the results of the study for a number of samples with different numbers of cycles associated with the fatigue damage.

Results of this study indicated a dynamic range of about 0.0020 with uncertainties of about 0.0003 as indicated by the range associated with the undamaged specimens which provide a measure of the uncertainties associated with the measurements. Consequently, the results indicated that it was relatively easy to detect damage accumulation essentially across the entire range from an unfatigued specimen through a failed specimen.

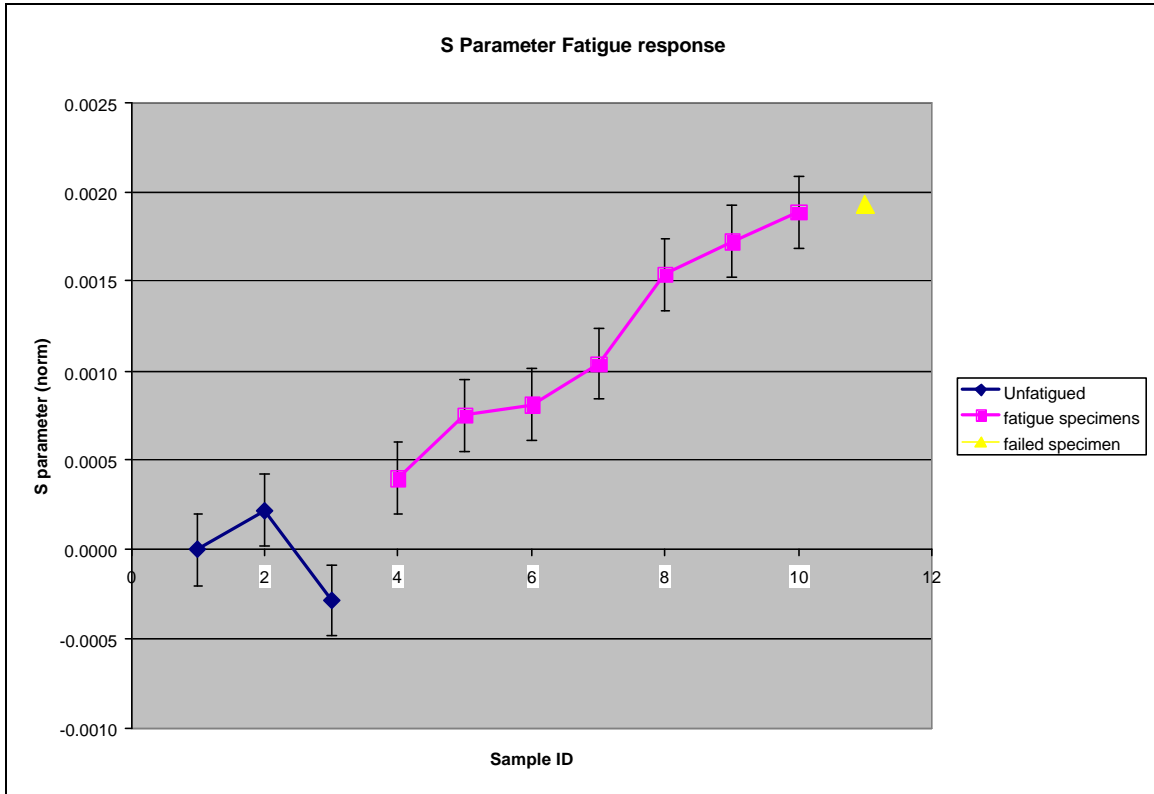


Figure 2. PIPA Fatigue Response

5.2 PIPA 2024 and 7075 Al Corrosion-Induced Fatigue Damage

PIPA measurements were performed on both blank and processed samples after corrosion testing and after each of the fatigue tests at 6000 and 11,000-12,000 cycles. Figure 3 shows the area measured on each specimen. This area is relatively small (0.2 in.²) but was used to provide a relatively localized response near the center of the specimen. The areas that can be examined range from about 0.1 in.² (1cm²) up to 4 in. x 4 in. Because corrosion does not deposit evenly, and the area being examined was relatively small (0.2 in²), it was expected that the PIPA response might be somewhat variable, as the distribution of corrosion damage on the samples appeared to be non-uniform. In hindsight, it would have been better to use a larger area collimator for these measurements to provide corrosion responses that were less variable.

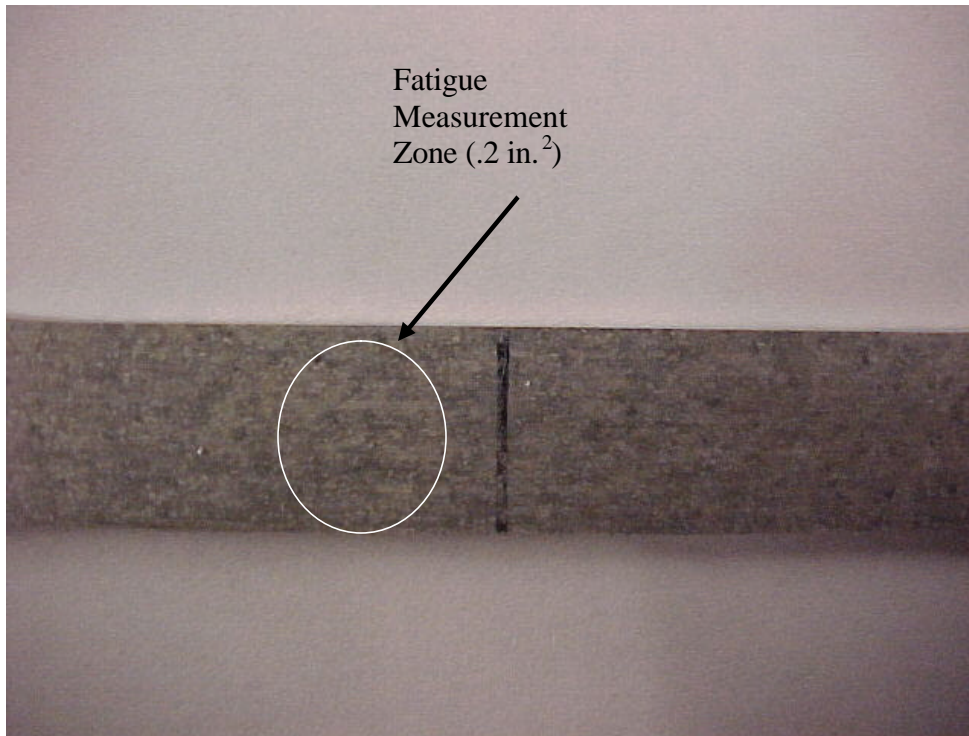


Figure 3. PIPA Analysis Area (0.5 in Diameter - .2 in²)

Initially, several series of measurements were performed to assess the variability of the PIPA response to possible random variations in the microstructure that is found in aluminum alloys. Table 9 lists a representative set of data that shows the variability of the results. In this case, the standard deviation of the average is about 0.00037. This is typically larger than the results seen in most reproducibility tests (0.0002) and may suggest that there are some variations in the microstructure that may affect the results. However, for this study these data provide a measure of the uncertainties that might be material induced. These data also provide the basis for comparisons with the corrosion and fatigue data.

Corrosion testing was performed as described in the previous sections. PIPA measurements were performed at the center of each coupon test section. Tables 10 and 11 list the PIPA results for the corrosion tests performed on 2024-T3 and 7075-T6 aluminum. The results shown are the S parameter result and peak to wing ratio (P/W ratio). In both cases, the results provide a measure of the change in lattice structure that may be induced by corrosion or fatigue damage. In some cases, the P/W ratio may be more sensitive to fatigue damage than is the S parameter.

Examination of the results in Table 10 for the 2024-T3 samples for the average PIPA response to the three levels of corrosion suggests that there might be an increase in response with increased corrosion. However, the uncertainties in the results generally overlap and suggest that for this alloy and the degree of corrosion exposure that the differences are not statistically defensible. If all sample results are averaged, and the standard deviation calculated, the result is 0.5441 with a standard deviation of 0.001. This suggests that the range is relatively narrow for these specimens (<0.2%), which suggests that the effect of direct corrosion on the 2024 at these

corrosion levels is not easily detectable. Some improvements have been made in the PIPA process since this time, which may improve the detectability of damage at this level.

Table 9. Reproducible Measurements of 2024 Blank Aluminum Specimens

| Specimen | File | S Parameter | Average | Standard Deviation |
|----------|-------|----------------|---------|-----------------------|
| 2-30 | Blank | 0.5398 | | |
| 2-31 | Blank | 0.5404 | | |
| 2-32 | Blank | 0.5403 | | |
| 2-30 | Blank | 0.5407 | 0.5404 | .00037 |
| 2-32 | Blank | 0.5407 | | |

In contrast, the results for the 7075-T6 samples (Table 11) produce a much more consistent response with considerably lower uncertainties at the higher corrosion level (96 hours), which may be due to the increased susceptibility of this alloy to corrosion damage. Figure 4 shows the average responses for the samples with different corrosion levels. In this case, the blank specimen has a much higher S parameter (0.0046 greater than the 24 hours response) than do any corrosion samples and is consistent with the blank measurement responses following fatigue testing. This difference between the blank and test specimens are considerably larger than that for the 2024 specimens and suggests that the difference between the blank and a corroded section may be used as a direct corrosion indicator. Further work needs to be done validate this although the results are consistent with the post fatigue measurements.

The second point that may be obtained from the results in Table 11 is that the response from the 96-hour group has a relatively low uncertainty and can be considered to be statistically different from both the 24-hour results and the blank specimen (which has a nominal standard deviation of .0004 based on prior reproducibility data). In contrast, the 24/24 specimens (48 hours total exposure) produce results that are similar to the 96-hour exposure data. This result might be expected based on the literature data, which suggests that corrosion causes the greatest degree of pitting on a fresh surface. These data would suggest that by exposing both surfaces that the integrated damage for both surfaces (24/24) is equivalent to that from a 96-hour exposure on one surface. Once validated, these data would suggest that PIPA can provide an integrated measure of corrosion damage in multi-layer structures although further measurements and measurements at higher corrosion levels are needed to reduce the uncertainties and to confirm that increased corrosion levels will continue to reduce the variability in the results.

5.3 2024 and 7075 PIPA Response to Corrosion Induced Fatigue Damage

This section summarizes the PIPA results for the 2024-T3 and 7075-T6 aluminum specimens that were performed after the samples had been subjected to 6000 cycles and after the next approximately 5000 cycles. Based on the literature data, the point in life for these specimens would likely be expected to be at the very low end of life as most specimens with the dimensions of the samples used would be expected to have nominal lives of greater than 100,000 cycles. As noted, issues with fabrication may have limited the life of these samples as those that failed essentially all failed near the end of the gage section.

Table 10. 2024 PIPA Corrosion Response

| Spectral ID | Sample ID | Corrosion Exposure (Hours) | S | | Standard deviation | P/W ratio | Average | Standard Deviation |
|-------------|-----------|----------------------------|-----------|---------|--------------------|-----------|---------|--------------------|
| | | | Parameter | Average | | | | |
| 906003 | 2-17 | No corrosion | 0.5449 | | | 2.3157 | | |
| 906004 | 2-20 | 24 | 0.5443 | 0.5435 | 0.001003 | 2.3117 | 2.2944 | .0133 |
| 906005 | 2-21 | 24 | 0.5437 | | | 2.2908 | | |
| 906006 | 2-22 | 24 | 0.5424 | | | 2.2807 | | |
| 906010 | 2-26 | 96 | 0.5450 | 5450 | | 2.3175 | 2.3175 | |
| 906007 | 2-23 | 24/24 | 0.5434 | 0.5443 | 0.001228 | 2.2940 | 2.3086 | .0170 |
| 906008 | 2-24 | 24/24 | 0.5437 | | | 2.3045 | | |
| 906009 | 2-25 | 24/24 | 0.5457 | | | 2.3272 | | |

Table 11. 7075 PIPA Corrosion Response

| Spectral ID | Sample ID | Corrosion Exposure (Hours) | S | | Standard deviation | P/W ratio | Average | Standard deviation |
|-------------|-----------|----------------------------|-----------|---------|--------------------|-----------|---------|--------------------|
| | | | Parameter | Average | | | | |
| 906015 | 7-17 | No corrosion | 0.5573 | | | 2.3618 | | |
| 906016 | 7-20 | 24 | 0.5536 | 0.5527 | 0.001292 | 2.3062 | 2.2931 | 0.0185 |
| 906018 | 7-22 | 24 | 0.5518 | | | 2.2800 | | |
| 906022 | 7-26 | 96 | 0.5546 | 0.5543 | 0.000325 | 2.3245 | 2.3155 | 0.0088 |
| 906023 | 7-27 | 96 | 0.5539 | | | 2.3150 | | |
| 906024 | 7-28 | 96 | 0.5543 | | | 2.3068 | | |
| 906019 | 7-23 | 24/24 | 0.5530 | 0.5536 | 0.000932 | 2.2936 | 2.3010 | 0.0107 |
| 906020 | 7-24 | 24/24 | 0.5546 | | | 2.3132 | | |
| 906021 | 7-25 | 24/24 | 0.5530 | | | 2.2961 | | |

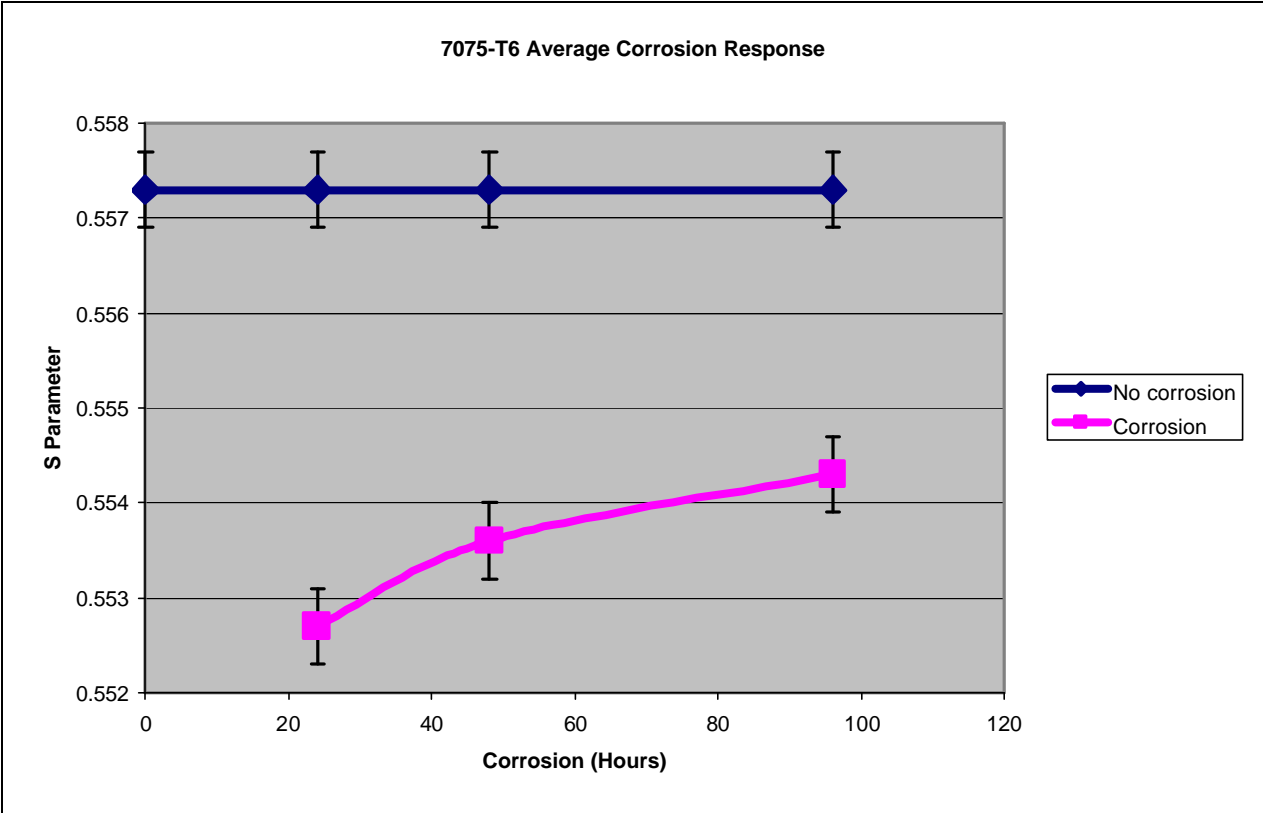


Figure 4. PIPA Response to Corrosion for 7075 Samples

Tables 12 and 13 present the PIPA response at 6000 cycles for the 2024-T3 and 7075-T6 specimens, respectively. In the case of the 2024-T3 data as shown in Figure 5, the 24 hour corrosion response is similar to that of the fatigued specimens without corrosion, whereas the 48(24/24) and 96 hour specimens still show a pronounced reduction below the blank specimen that is consistent with the pure corrosion response in Table 10. However, the difference between the non-corroded and fatigued specimens has gotten much larger. The pure corrosion results were statistically the same whereas the difference between the fatigued specimen and corroded 48 and 96 hours specimens has increased to about 0.0026. Why the higher levels of corrosion damage should inhibit some of the PIPA response to fatigue damage is unclear; however, as will be discussed, the response for the high corrosion specimens increases more rapidly after the second fatigue series and becomes similar to the damage for the fatigued and 24 hour specimens. The uncertainties on this data for the corrosion specimens range from about 0.0002 to 0.0005, indicating good reproducibility.

Figure 6 shows the results for 7075-T6 specimens. In this case, there is a monotonic increase from the 24-hour through the 96-hour corrosion specimens with the 96-hour S parameter response becoming closer to that from the blank and pure fatigue damage. If it is assumed that the 7075-T6 is more susceptible to pitting, which acts as stress concentrators in the material, the increased response would be due to the production of higher levels of fatigue in these samples relative to the more corrosion resistant 2024 samples.

Table 12. 2024 Aluminum Exposed to Corrosion and 6000 Fatigue Cycles

| Spectral ID | Sample ID | Description | Corrosion Exposure (Hours) | S | | P/W ratio | Average | S.D. | |
|-------------|-----------|------------------------------|----------------------------|-----------|---------|-----------|---------|--------|--------|
| | | | | Parameter | Average | | | | |
| 912010 | 2-30 | Blank | | 0.5398 | | 2.2417 | | | |
| 912011 | 2-31 | Blank | | 0.5404 | | 2.2536 | | | |
| 912012 | 2-32 | Blank | | 0.5403 | | 2.2537 | | | |
| 912013 | 2-30 | Blank | | 0.5407 | 0.5404 | 0.0004 | 2.2570 | 2.2539 | 0.0079 |
| 912015 | 2-32 | Blank | | 0.5407 | | | 2.2634 | | |
| 912016 | 2-17 | NC -6000 C | | 0.5404 | 0.5413 | 0.0008 | 2.2588 | 2.2701 | 0.0098 |
| 912017 | 2-18 | NC -6000 C | | 0.5419 | | | 2.2760 | | |
| 912018 | 2-19 | NC -6000 C | | 0.5415 | | | 2.2755 | | |
| 912019 | 2-20 | 6000 C | 24 | 0.5414 | 0.5409 | 0.0005 | 2.2732 | 2.2694 | 0.0053 |
| 912020 | 2-21 | 6000 C | 24 | 0.5410 | | | 2.2715 | | |
| 912021 | 2-22 | 6000 C | 24 | 0.5404 | | | 2.2634 | | |
| 912025 | 2-26 | 6000 C | 96 | 0.5388 | 0.5387 | 0.0002 | 2.2334 | 2.2313 | 0.0041 |
| 912026 | 2-27 | 6000 C | 96 | 0.5386 | | | 2.2273 | | |
| 912027 | 2-28 | 6000 C | 96 | 0.5383 | | | 2.2284 | | |
| 912028 | 2-29 | 6000 C- broken at edge | 96 | | | | | 2.2360 | |
| 912022 | 2-23 | 6000 C | 24/24 | 0.5391 | 0.5393 | 0.0004 | 2.2472 | 2.2442 | 0.0094 |
| 912023 | 2-24 | 6000 C | 24/24 | 0.5398 | | | 2.2517 | | |
| 912024 | 2-25 | 6000 C | 24/24 | 0.5391 | | | 2.2336 | | |

Table 13. 7075 Aluminum Exposed to Corrosion and 6000 Fatigue Cycles

| Spectral ID | Sample ID | Description | Corrosion Exposure (Hours) | S | | P/W ratio | Average | S.D. | |
|-------------|-----------|--------------------|----------------------------|--------|---------|-----------|---------|--------|--------|
| | | | | Param. | Average | | | | |
| 913004 | 7-32 NC | Blank | | 0.5708 | | 2.7670 | | | |
| 913005 | 7-17 | NC -6000 C | | 0.5710 | 0.5703 | 0.00092 | 2.7658 | 2.7574 | 0.0144 |
| 913006 | 7-18 | NC -6000 C | | 0.5707 | | | 2.7656 | | |
| 913007 | 7-19 | NC -6000 C | | 0.5693 | | | 2.7408 | | |
| 913008 | 7-21 | 6000C | 24 | 0.5675 | 0.5668 | 0.00095 | 2.6991 | | |
| 913009 | 7-22 | 6000 C | 24 | 0.5661 | | | 2.6790 | | |
| 913013 | 7-26 | 6000 C | 96 | 0.5692 | 0.5689 | 0.00052 | 2.7235 | 2.7249 | 0.0102 |
| 913014 | 7-27 | 6000 C | 96 | 0.5692 | | | 2.7358 | | |
| 913015 | 7-28 | 6000 C | 96 | 0.5683 | | | 2.7154 | | |
| 913016 | 7-29 | 6000 C | 96 | 0.5676 | | | 2.7061 | | |
| 913018 | 7-30 | 29000 C 6000 C- | 0 24 | 0.5677 | | | 2.7084 | | |
| 913017 | 7-20 | Broken | | 0.5690 | | | 2.7237 | | |
| 913010 | 7-23 | 6000 C | 24/24 | 0.5673 | 0.5683 | 0.00087 | 2.6994 | 2.7154 | 0.0147 |
| 913011 | 7-24 | 6000 C | 24/24 | 0.5686 | | | 2.7185 | | |
| 913012 | 7-25 | 6000 C | 24/24 | 0.5690 | | | 2.7285 | | |

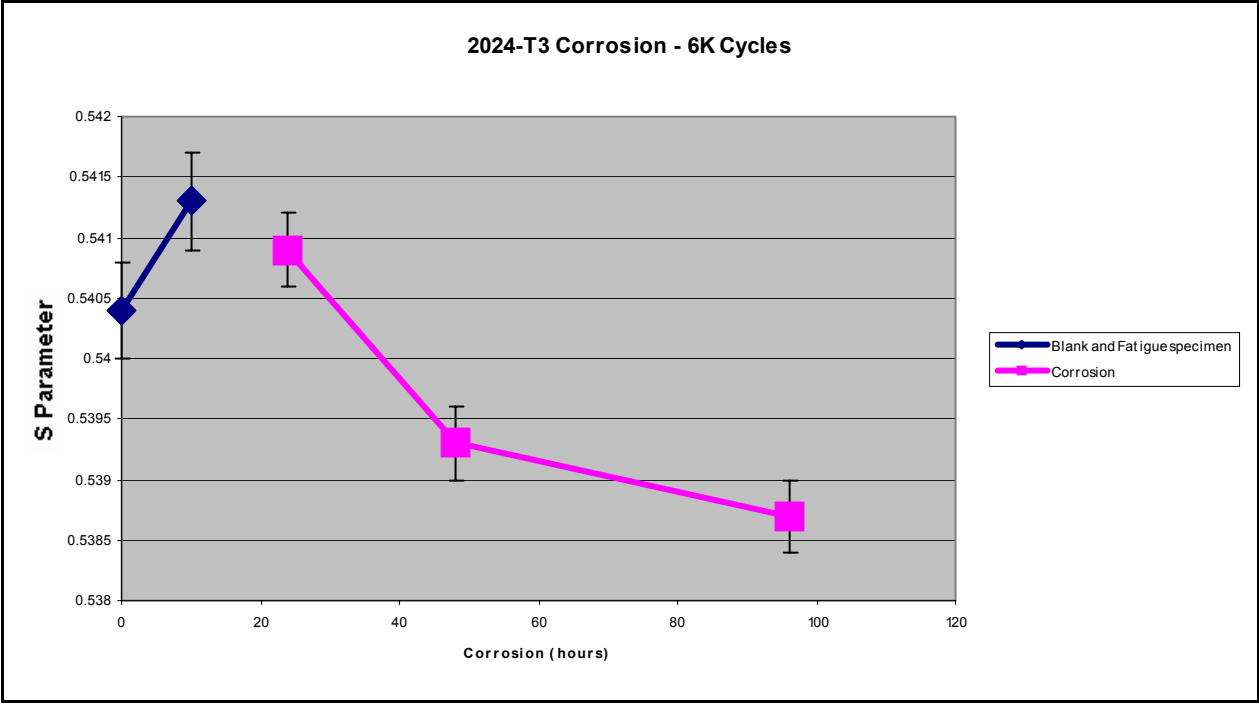


Figure 5. 2024 Fatigue Damage at 6000 Cycles

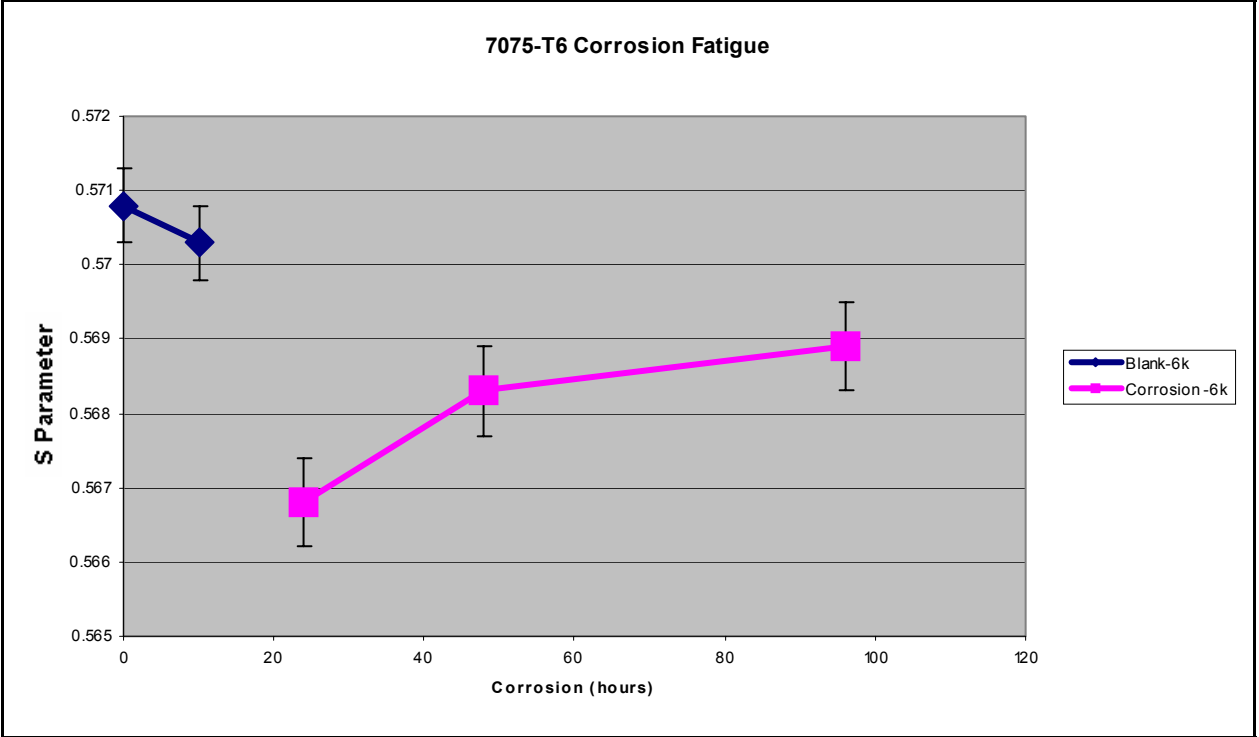


Figure 6. 7075 Fatigue Damage at 6000 Cycles

Figure 7 shows the 2024-T3 measurements at 6000 and 12000 cycles. The results indicate a change in the behavior of the higher corrosion samples with a significant shift upward in the fatigue damage response. This response is statistically significant for the higher corrosion levels, which show a significant change. Although the error bars for this data set are not as good as some of those for the 7075 results, which appear to be producing more consistent data.

Table 8 shows the comparison between the 6000 and 12000 cycle data for the 7075-T6 samples. In this case, there appears to be a consistent offset for data at 12000 cycles and with relatively small uncertainties (0.0002 - 0.0006) for the data from the corrosion specimens. These data would suggest that at 6000 cycles the fatigue damage for the corroded samples was less than would be expected for a sample without corrosion damage, but that after that point the corroded samples appear to be fatiguing at a faster rate with a significantly greater increase in overall damage. This rate is also considerably higher than that observed for the 2024 specimens. In this case, data were used from samples that fractured prior to reaching 11000 cycles. We believe these failures were likely due to misalignment of the fatigue test machine or poor sample cutting. We also believe that if the samples had lasted until 11000 cycles, the average differences may have been greater than those observed.

In summary the results that have been obtained to date indicate the following:

- The presence of corrosion both on the surface and in buried layers results in a detectable change in the PIPA response and that it appears to correlate with the extent of the corrosion damage to which the material was subjected either on a single or on a multi-layer surface.
- Corrosion damage produces a measurable response that is below the response of either a non-corroded specimen or a fatigued specimen.
- Corrosion damage in the 7075 specimens appear to be more severe than that in the 2024 specimens as might be expected from the literature.
- In general, there appears to be monotonic increase in the PIPA fatigue damage response for the 7075 specimens and a lesser although measurable response for the 2024 specimens.

In all cases, it should be noted that this is an initial feasibility assessment of a new technology on relatively low levels of corrosion and fatigue damage. The results suggest that both corrosion and fatigue damage are detectable. Further work is needed to optimize the measurement process and to better understand the mechanisms involved. The current results should be correlated with both SEM and X-ray diffraction analysis to assess the PIPA response relative to the microstructural changes that are occurring. Further, improvements are needed in the sample preparation and fatigue testing process. Also it should be pointed out that these measurements were performed before substantial improvements in the stability and reproducibility of the PIPA measurement system used for these measurements.

Table 14. 2024 Aluminum Exposed to Corrosion and up to 12,000 Fatigue Cycles

| Spectra IID | Sample ID | Descrip | Corrosion Exposure (Hours) | S Param. | Ave. | S.D. | P/W ratio | Ave. | S.D. |
|------------------------|----------------------|----------------|---|-----------------|-------------|-------------|------------------|-------------|-------------|
| 925005 | 2-30 | Blk | 0 | 0.5665 | | | 2.7255 | | |
| 925006 | 2-17 | 11K C | 0 | 0.5676 | 0.5663 | 0.0011 | 2.7597 | 2.7368 | 0.0204 |
| 925007 | 2-18 | 11K C | 0 | 0.5653 | | | 2.7205 | | |
| 925008 | 2-19 | 11K C | 0 | 0.5662 | | | 2.7302 | | |
| 925009 | 2-20 | 11K C | 24 | 0.5662 | 0.5651 | 0.0010 | 2.7273 | 2.7122 | 0.0132 |
| 925010 | 2-21 | 11K C | 24 | 0.5647 | | | 2.7027 | | |
| 925011 | 2-22 | 11K C | 24 | 0.5643 | | | 2.7067 | | |
| 925012 | 2-31 | | | 0.5654 | | | 2.7226 | | |
| 925013 | 2-23 | 11K C | 24/24 | 0.5677 | 0.5667 | 0.0009 | 2.7526 | 2.7405 | 0.0105 |
| 925014 | 2-24 | 11K C | 24/24 | 0.5665 | | | 2.7353 | | |
| 925015 | 2-25 | 11K C | 24/24 | 0.5659 | | | 2.7336 | | |
| 925016 | 2-26 | 11K C | 96 | 0.5672 | 0.5664 | 0.0009 | 2.7435 | 2.7334 | 0.0171 |
| 925017 | 2-27 | 11K C | 96 | 0.5654 | | | 2.7137 | | |
| 925018 | 2-28 | 11K C | 96 | 0.5666 | | | 2.7430 | | |
| 925019 | 2-29 | 13225 | 0 | 0.5665 | | | 2.7363 | | |
| 925020 | 2-32 | Blk | 0 | 0.5660 | | | 2.7208 | | |

Table 15. 7075 Aluminum Exposed to Corrosion and up to 12,000 Fatigue Cycles

| Spectra IID | Sample ID | Descrip | Corrosion Exposure (Hours) | S Param. | Ave. | S.D. | P/W ratio | Ave. | S.D. |
|------------------------|----------------------|----------------|---|-----------------|-------------|-------------|------------------|-------------|-------------|
| 924003 | 7-31 | Blank | | 0.5712 | | | | | |
| 924004 | 7-17 | 12k | 0 | 0.5703 | 0.5712 | 0.0008 | 2.7671 | 2.7792 | 0.0174 |
| 924005 | 7-18 | 12k | 0 | 0.5719 | | | 2.7991 | | |
| 924006 | 7-19 | 12k | 0 | 0.5715 | | | 2.7714 | | |
| 924007 | 7-20 | 6946-F | 24 | 0.5709 | 0.5711 | 0.0002 | 2.7663 | 2.7717 | 0.0094 |
| 924008 | 7-21 | 11K | 24 | 0.5711 | | | 2.7662 | | |
| 924009 | 7-22 | 11K | 24 | 0.5712 | | | 2.7825 | | |
| 924013 | 7-26 | 11K | 96 | 0.5711 | | | 2.7727 | | |
| 924014 | 7-27 | 9400-F | 96 | 0.5729 | 0.5721 | 0.0004 | 2.8023 | 2.7903 | 0.0103 |
| 924015 | 7-28 | 9060-F | 96 | 0.5722 | | | 2.7849 | | |
| 924016 | 7-29 | 14350-F | 96 | 0.5720 | | | 2.7838 | | |
| 924010 | 7-23 | 7297-F | 24/24 | 0.5727 | 0.5725 | 0.0006 | 2.8078 | 2.8000 | 0.0077 |
| 924011 | 7-24 | 8899-F | 24/24 | 0.5730 | | | 2.7997 | | |
| 924012 | 7-25 | 8562 | 24/24 | 0.5719 | | | 2.7924 | | |

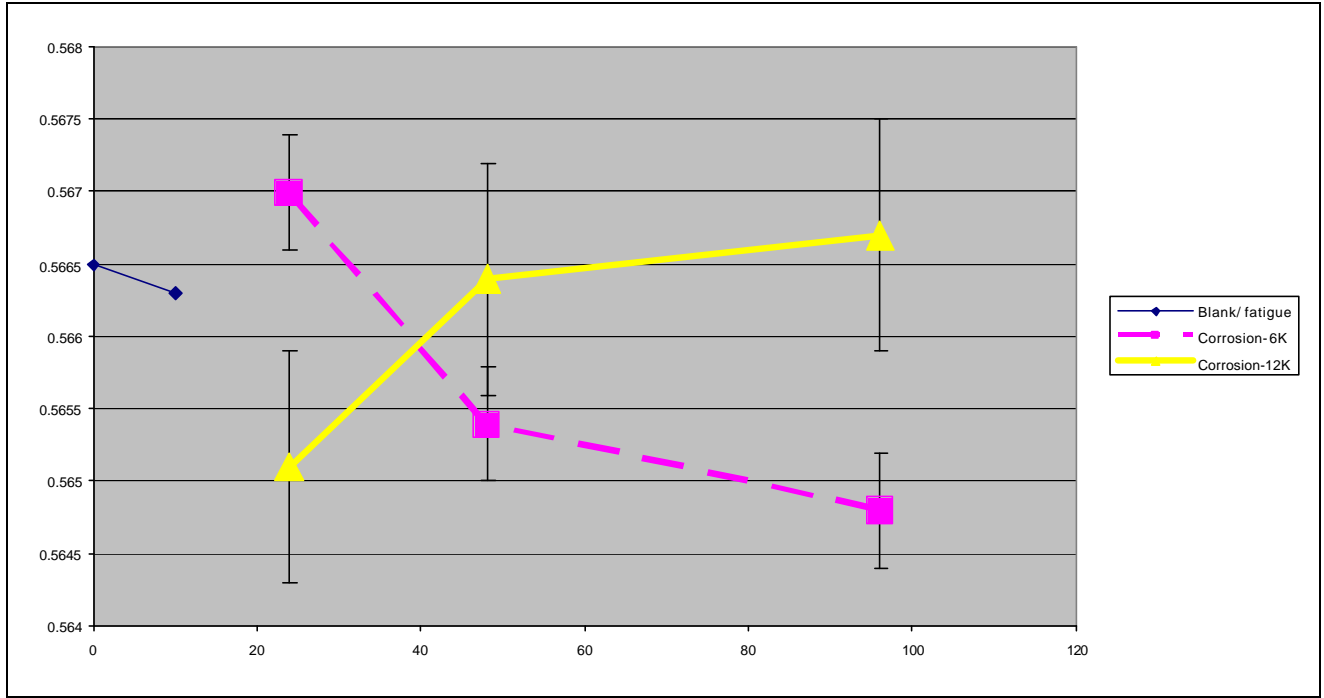


Figure 7. 2024 Damage after 11000 Cycles

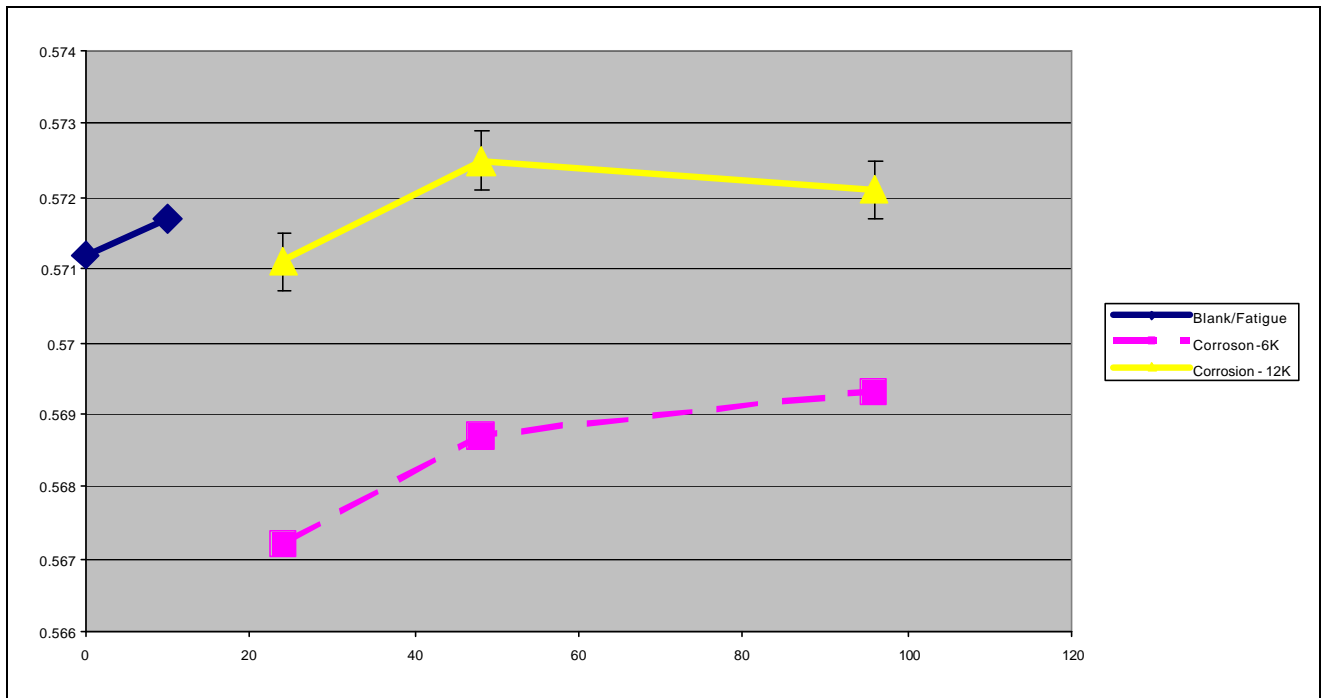


Figure 8. 7075 Damage after 6000 and 11000 Cycles

6.0 CONCLUSIONS

Corrosion and corrosion-induced fatigue damage are critical issues for aircraft life extension and CBM. For PIPA measurement data to have an impact on these issues, two types of applications have been identified. First is to use the PIPA technology to develop fatigue damage algorithms with appropriate reliability measures (or uncertainties) that can be implemented. This requires that PIPA must be able to detect and accurately quantify fatigue damage with suitable uncertainties and to be able to implement these in quantifiable models. The second is to utilize the PIPA technology or one of its associated technologies, Neutron Induced Positron Annihilation, (NIPA) or the On Line Positron Monitor (OLPM) for performing periodic damage assessments to determine the probability of the component or aircraft for reaching its next inspection. The objective is primarily to address the first potential application of this technology. The second would be a straightforward application of the first using either the direct PIPA technology or the smaller, less-sophisticated systems.

To reach the first goal requires that the technology must be able to detect the phenomena involved, be accurate and have sufficiently small uncertainties that it can provide an adequate measurement of remaining life or the probability that the part will reach the next inspection. This study of the PIPA technology was performed to provide an initial assessment of whether the various phenomena involved in corrosion-induced fatigue were detectable and quantifiable. Although there were problems associated with the sample preparation, corrosion testing, and fatigue testing, the results do indicate that a number of the phenomena involved are detectable and at relatively low levels of likely corrosion or fatigue damage. In addition, since the time when these measurements were performed, the stability and reproducibility of the PIPA process has been improved.

Based on the PIPA results to date, both corrosion and corrosion-induced fatigue are detectable on single or multilayer surfaces; although, the uncertainties and the microstructural changes that are being detected are not yet well defined. Further, the data indicate that the difference between alloys that are more or less sensitive to corrosion can be detected and quantified. It should be noted that further work is needed to validate the results where the sample preparation and processing uncertainties are reduced and measurement uncertainties are improved.

The PIPA response due to the presence of corroded material that may include stress corrosion cracking (SCC) results in a reduction of the PIPA response that appears to correlate with the extent of the corrosion (i.e., 7075-T6 more corroded than 2024-T3). As direct corrosion layers on the metal surfaces are typically 20 micron or less for the exposure periods involved, the PIPA results would suggest deeper changes in the material that can affect the remaining life of the material. In the case of 7075-T6, the presence of corrosion in other studies has been shown to reduce remaining life by a factor of 6-8, consequently, it appears that the corrosion does result in more significant effects on the material than can be accounted for by a relatively thin corrosion layer. Further studies including comparisons with SEM and X-ray diffraction analysis are needed to better understand this issue and the correlation with the PIPA response.

In the case of the PIPA fatigue analysis results, the results suggest that initially the corrosion changes the material properties as indicated by the fact that the PIPA response during the initial

fatigue cycle are below that for uncorroded fatigued samples, but that after some initial period the fatigue response becomes more significant with the damage becoming similar to the uncorroded samples and in the case of the 7075-T6 data exceeding the damage measured for the uncorroded samples. The data suggests that the presence of corrosion speeds up the effect of fatigue damage on the material as might be expected.

The primary objective of these summaries is to provide the basis for applying these data to a process for using these data in the development of fatigue damage algorithms. Obviously, the simplest process is to detect either single or multilayer corrosion. The results indicate a significant and quantifiable reduction in the S parameter with corrosion relative to a section of virgin material. The approach taken would be to perform measurements on potentially corroded areas away from stress concentrators, such as fastener holes, and assess the response at these locations and compare it with the response of both virgin material and standards of that type that had been corroded to several levels to validate the response. This approach should provide a direct measure of integrated corrosion damage within a range where appropriate uncertainties can be defined. It is expected that a relatively simple model that correlates measurable corrosion damage for a given thickness of material with the response for a blank specimen and specimens with varying damage and specimen thickness can be developed. The PIPA response would be compared with SEM and other data to develop these algorithms to provide a numerical measure of corrosion damage.

In the case of corrosion-induced fatigue, the process would be most effective at locations where cracks are expected to start (e.g., fastener holes). These stress concentrators would provide a good measure of the buildup of corrosion damage relative to other fastener holes that are subjected only to fatigue damage. In any event, the corrosion-induced fatigue may likely have the same endpoint PIPA response as the direct fatigue damage but would likely be at a higher level than the for direct fatigue for the same number of operational cycles as suggested by the data to date. The model developed for this process would involve a correlation with the blank specimen and samples of fatigued and uncorroded material to develop a response curve for the damage effects. This fatigue damage curve would likely be enhanced with operational samples with known periods of life or that had failed from corrosion-induced fatigue.

This initial study provides a number of implications concerning further work needed to utilize the PIPA technology for measuring corrosion-induced fatigue. As demonstrated in the work shown, PIPA can quantify fatigue damage at levels down to the as manufactured material and that the technique is not significantly affected by variations in the composition of the aluminum alloys, which do have variable compositions to some degree, as demonstrated by the reproducibility of the measurements performed. Further measurements are needed at higher stresses and with better-prepared samples to better define the effects of the damage. Also, work with actual holes similar to those found in wing lap splices should be performed to better concentrate the stress and allow the corrosion damage effects to be better defined.

7.0 PHASE II WORK PLAN

The Phase II work plan provides the structure of the follow on work needed to develop this technology into a process that is usable for developing accurate reliability algorithms and to begin development of a process that could be used in a field environment. A detailed Phase II work plan has been prepared; however, some of the principal elements of this plan should be restated. These elements include the following:

- Perform additional studies with improved samples and testing to better assess the uncertainties associated with the direct measurement of corrosion and the corrosion-induced PIPA response. Further the process should be validated for all primary aluminum alloy types used in applications where catastrophic failure could result.
- Perform measurements on samples that are prepared to specifications as close to real world samples as possible. This may include lap splice joint with fastener holes and actual corrosion damage.
- Perform measurements on specimens with different thicknesses so that the PIPA response can be correlated with corrosion.
- Develop actual fatigue algorithms that can be accurately correlated with both sample measurements and measurements performed on operational samples from all stages of life and failed.
- Characterize the smaller systems, NIPA and the on line monitor so that they can be used for field measurements.

Development of this technology through this process should provide usable algorithms with uncertainties that combined with depot level measurements should provide a program that will be usable to assess remaining performance life or the probability of failure prior to the next inspection.

8.0 REFERENCES

1. Lichtenwaler, Peter F.; White, Edward V.; and Baumann, Erwin W.; "Information processing for aerospace structural health monitoring," *Proceedings of SPIE – the International Society for Optical Engineering, Smart Structures and Materials 1998 – Industrial and Commercial Applications of Smart Structures Technologies*, Vol. 3326, pp. 406-417, 1998.
2. McDowell, D.L.; Clayton, J.D.; and Bennett, V.P.; "Integrated diagnostic/prognostic tools for small cracks in structures," *Proceedings of the Institution of Mechanical Engineers, Part C – Journal of Mechanical Engineering Science*, Vol. 214, no. 9, pp. 1123-1140, 2000.
3. Kelly, R., Scully, J., Altynovas, M., Peeler, D. T., Combining Probabilistic and Database Approaches to the Prediction of Corrosion Damage in Aging Aircraft, *Fifth Joint NASA/FAA/DOD Conference on Aging Aircraft*, Orlando Florida, September 9/ 2001.
4. Falugi, M., Tuegel, E., Brooks, C., Bell, R., Shelton, D., "Comparison of the Corrosion/Fatigue Effects on Sealed and Unsealed Longitudinal Fuselage Splices," *Fifth Joint NASA/FAA/DOD Conference on Aging Aircraft*, Orlando Florida, September 9/ 2001.
5. Brooks, C.L.; Peeler, D.T.; Honeycutt, K.T.; and Prost-Domasky, S.; "Predictive Modeling for Corrosion Management: Modeling Fundamentals," *Proceedings of the Third Joint FAA/DoD/NASA Conference on Aging Aircraft (A00-1150101-01)*, Albuquerque, NM, 20-23 Sept. 1999.
6. Brooks, C.L.; Peeler, D.T.; Honeycutt, K.T.; and Prost-Domasky, S.; "Predictive Modeling for Corrosion Management: Modeling Fundamentals," *Proceedings of the Third Joint FAA/DoD/NASA Conference on Aging Aircraft (A00-1150101-01)*, Albuquerque, NM, 20-23 Sept. 1999.
7. Bray, G. H., et. al., "Effects of prior corrosion on the S/N fatigue performance of aluminum alloys 2024-T3 and 2524-T3," *Effects of Environment on the Initiation of Crack Growth*, ASTM STP 1298, ASTM, Philadelphia 1992, pg 20.
8. Sankaran, K., "Effects of Pitting Corrosion on the Fatigue Behavior of Aluminum Alloy 7075-T6: Modeling and Experimental Studies," *Materials Science and Engineering*, A 297 (2001), pp. 223-229.
9. Bray, G. H., et. al., "Effects of prior corrosion on the S/N fatigue performance of aluminum alloys 2024-T3 and 2524-T3," *Effects of Environment on the Initiation of Crack Growth*, ASTM STP 1298, ASTM, Philadelphia 1992, pg 20.
10. Pantelakis, Sp.G., "Tensile and Energy Density Properties of 2024, 6013, 8019 and 2091 aircraft aluminum alloy after corrosion exposure," *Theoretical and Applied Fracture Mechanics*, 33(2000) 117-134.

11. Chen, G. S., Transition from pitting to fatigue crack growth- modeling of corrosion fatigue crack nucleation in a 2024-T3 aluminum alloy,” *Materials Science and Engineering*, A219 (1996) 126-132.
12. Staab, T.E.M., et. al., “Positron Lifetime measurements for characterization of nano structural changes in the age hardenable alloy “AlCuMg 2024 alloy,” *Journal of Material Science*, 35 (2000) 4667-4672.
13. Dlubek, G., et. al., Positron Lifetime Studies of Decomposition in 2024 (Al-Cu-Mg) and 7010 (Al-Zn-Cu-Mg) Alloys, *Scripta Materiala*, Vol 39, No. 7 pp 893-898, 1998.
14. Shultz, Peter, and Lynn, K.G., *Interaction of Positron Beams with Surfaces*, Thin Films, and Interfaces, *Reviews of Modern Physics*, Vol 60, No 3 July 1988.
15. Gauster, W.B., et. al., *A study of deformation Fatigue of 316 Stainless Steel at Room Temperature by Positron Annihilation*. NUREG CR/0118, 1978
16. Niskiwaki, K. et. al., *The study of Fatigued Stainless Steel by Positron Annihilation, Proceedings of the Fifth International Conference on Positron Annihilation*, Japan Institute of Metals pp 1121-1131, 1979.
17. Szeles, C. and Lynn, K. G., *Positron-Annihilation Spectroscopy*, *Encyclopedia of Applied Physics*, Volume 14.
18. Jean, Y.C., *Characterizing Free Volumes and Holes in Polymers by Positron Annihilation Spectroscopy*, NATO Advanced Research Workshop, Advances with Positron Spectroscopy of Solids and Surfaces. Varenna Italy, July 16-17, 1978.
19. Grobstein, L., et. al., *Fatigue damage accumulation in nickel prior to crack initiation*, *Science and Engineering A138* (1991) 191-203.

APPENDIX A

Introduction

The following technical explanation is a detailed discussion on the principles of positron annihilation that have been studied and proven over the last 40 years during the extensive research conducted in positron beam spectroscopy. Photon Induced Positron Annihilation (PIPA) achieves the same positron annihilation reactions depicting lattice structure damage at the atomic level; however, PIPA is much more sensitive and accurate because it is not hindered by surface interference, such as coatings or corrosion, nor component geometry, both of which limited the depth and accuracy of positron beam spectroscopy.

Technical Discussion of the PIPA Concept

The PIPA technology applied in this research is a process recently developed and patented at the Idaho National Engineering and Environmental Laboratory (INEEL). This technology is a new addition to material characterization technologies that has a number of specific applications to almost all materials industries. PIPA extends the current limited use of positron annihilation measurement technology to a much broader range of applications, allowing the technique to be used as a more general-purpose, nondestructive assay technique.

Specific improvements developed at INEEL and incorporated in this technology are:

- Use of high-energy photons (15-20 MeV) to generate neutron deficient nuclei in materials (e.g., most metals, composites and polymers) that in many cases produce positrons within bulk material that allow bulk fatigue or lattice structure change/damage to be measured in either a research or process measurement environment.
- Use of digital data acquisition electronics that allow highly reproducible, stable gamma spectrometry and positron lifetime measurements to be made to assess bulk defects or the characteristics of various inclusions in the metals or other materials.
- Portable gamma spectrometry measurement systems and linear accelerators that can be easily transported for use in either field or manufacturing facility environments.

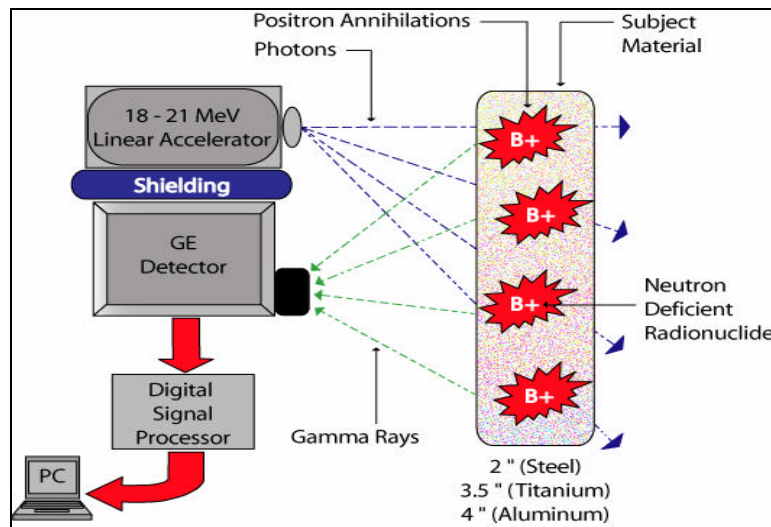
PIPA techniques have shown remarkable potential in the identification and measurement capabilities for material assessment that include:

- Identify atomic lattice defects <10 microns in size.
- Measurement uncertainties on the order of less than 1%.
- Multi-layer defect detection in metals and composites.
- Cross-sectional analysis.
- Assess lattice structure change/damage at less than 1%. Crack initiation/loss of plasticity = 100%.

The PIPA process generates positrons deep within the bulk material through the application of high-energy X-ray bombardment of the target material. Positrons are formed when the X-rays cause a neutron to be ejected from a material's atom (photo-neutron reaction) and the resultant atomic isotope decays into a more stable material through positron decay. This is a revolutionary

advancement over previous positron beam spectroscopy where the positron penetration and defect detection depths were significantly limited and impacted by surface characteristics. The positrons created by the PIPA process are formed throughout the bulk material, achieving a better sensitivity and accuracy level of defect detection than positron beam spectroscopy. The depth of defect detection for PIPA is only limited by the attenuation of the annihilation gammas to be measured by the germanium detector; related to the material density. This depth is 2 inches in iron, 3.5 inches in titanium, and up to 4 inches in aluminum, which can be doubled with two detectors and access to both sides of the material/component. Figure A1 illustrates the basic operating model and functional procedure of PIPA.

Figure A1. Photon Induced Positron Annihilation Process



Positron Annihilation Theory

A positron is a charged particle equal in mass to an electron, but with a positive charge equal in magnitude but opposite to the negative charge of the electron. When positrons are created in materials, the positrons rapidly lose most of their kinetic energy by collisions with ions and free electrons. An energetic positron created inside of a solid is slowed down to thermal energies within about 10 ps ($1 \text{ ps} = 10^{-12} \text{ s}$). Upon thermalization, the positrons diffuse away from the point where they are thermalized, until they finally annihilate with an electron. During this diffusion process, the positrons are repelled by positively charged nuclei (protons) and thus seek defects such as dislocations in the lattice sites, where the concentration of nuclei charge density is lower.

A thermalized positron has a typical mean velocity of 10^5 m/s . The balance between the diffusion rate (after thermalization) and the annihilation rate of thermalized positrons is such that on average, each positron has time to diffuse just a few tens of a micrometer from its point of thermalization. The typical mean lifetime and the total distance traveled by a thermalized positron before it annihilates with an electron are 200 ps and 20 μm , respectively. The distance ($\sim 20 \mu\text{m}$) traveled after thermalization encompasses about 10^5 lattice sites, providing a good chance that the positron will encounter a defect and be trapped; even if the defects are present in

fairly small concentrations. (10 parts per million of defects ensures that on average there is one defect for every 10^5 lattice sites).

Defects in materials occur over a wide range of mechanisms, as shown in Figure A2. At the smallest scale, defects consist of single missing atoms (or vacancies) in the material. At higher defect concentrations, the vacancies may connect into dislocations; the first stage toward what may become a crack. Larger defects with no material in them are called voids. In polymers, which are made up of long molecules, defects may aggregate between molecules and form microscopic holes. Figure A3 depicts the formation and subsequent thermalization of the positron as it travels through the lattice sites, searching for a lower charge density region, (defected area), becoming trapped and then annihilated.

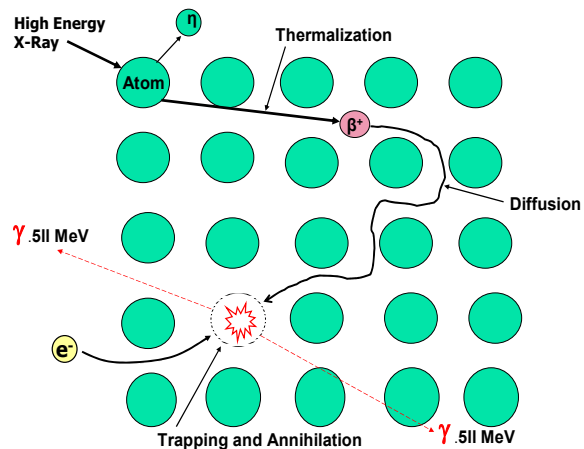
Complete annihilation of both particles occurs when a positron encounters an electron and their mass is converted into pure energy in the form of two gamma rays. If the positron and the electron with which it annihilates were both at rest at the time of decay, the two gamma rays would be emitted in exactly opposite directions (180 degrees apart), in accordance with the principle of conservation of momentum. Each annihilation gamma ray would have energy of 0.511 MeV, the rest energy of an electron and of a positron. A thermalized positron, trapped in a defected area is essentially at rest, unlike the electrons.

Figure A2. Defect Characterization

| Defect Type | Size | Materials |
|------------------|------------------|----------------------|
| Atomic Vacancies | .1 nm | Metals |
| Dislocations | 1 nm-10 μ m | Metals |
| Voids | .1 nm-1 μ m | Metals Composites |
| Holes | .1 nm-10 μ m | Polymers |

LLNL

Figure A3. Positron Lifecycle



The momentum of the electrons determines the additional impact of the momentum energy to the electron-positron at-rest annihilation gamma energy of 0.511 MeV. The added momentum of the electron causes the direction of the annihilation gamma rays to deviate from the nominal value of 180 degrees. Likewise, the energy of the annihilation gamma rays deviates slightly from 0.511 MeV, depending on the momentum of the electrons, because of the Doppler effect. Three key characteristics of positrons and the radiation that they emit upon annihilation with electrons make the positron annihilation method highly useful for detecting the presence and size of microscopic flaws in materials.

- First, the positrons' positive electrical charge causes them to be repelled by protons. This characteristic accounts for their attraction to dislocations, vacant lattice sites, vacancy

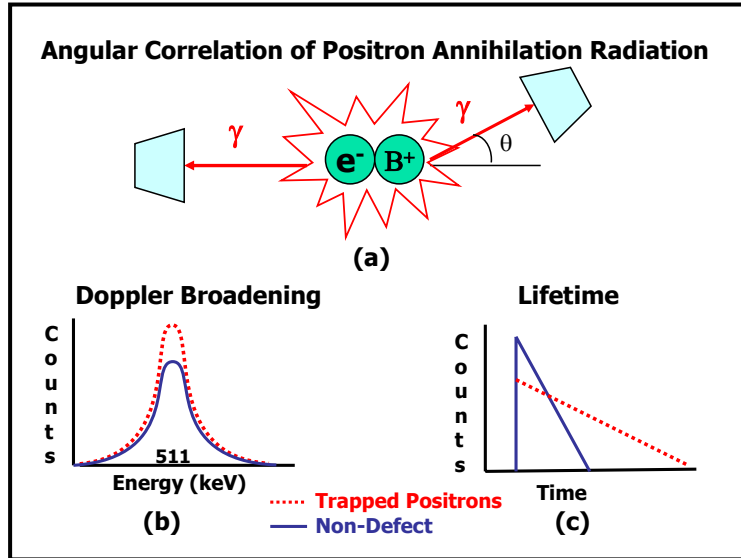
clusters, cavities, and other open volumes (voids) in the material, where the density of atomic nuclei is lower. Thus, a small increase in the number or size of the microscopic defects in a sample results in a large increase in the proportion of annihilation events occurring in the defects.

- Second, the annihilation radiation is sensitive to the momentum distribution of the electrons with which positrons annihilate. Defects contain a higher ratio of free electrons to core electrons than non-defected materials. This phenomenon can be explained by the tendency of free (conduction) electrons to spill over into the defect more than core electrons. Core electrons have a much higher linear momentum than do free electrons. Thus, gamma rays from annihilation events involving free electrons are more likely to approximate the energy (0.511 MeV) and direction (180 degrees) typical of gamma rays produced by events involving positrons and electrons at rest. These characteristics make it possible to detect the presence of defects from the energy spectrum of the gamma ray emissions and from the spectrum of angles of deviation from 180 degrees.
- Third, because the density of electrons is lower in defected material than in non-defected material, the mean lifetime of thermalized positrons trapped in defects is longer than those diffusing in perfect material. Within a few picoseconds after the positron is injected into the material, the nucleus (in the source) emits an energetic, prompt gamma ray (1.28 MeV in the case of a “Na” source) that serves as a birth signal. The lifetime of the positron can be measured as the time elapsed between the birth and annihilation gamma rays. Thus, measurement of positron lifetimes can also be used to indicate the presence of defects in the material.

Measurement of the gamma ray angles (angular correlation), energy spectrum (Doppler broadened line-shape), and positron lifetime will determine whether the positrons are interacting with free electrons in defected areas or core electrons in the bulk material. Those measurements are illustrated in Figure A4.

Figure A4 (a) illustrates measurement of the distribution of angles between two annihilation gamma rays about the nominal value of 180 degrees. This deviation from colinearity between two 0.511 MeV annihilation gamma rays is a product of the momentum of the annihilating electron. Less deviation from colinearity indicates the presence of defects. The electron momentum also produces a Doppler shift in the 0.511 MeV gamma annihilation radiation, and this shift can be seen in an accurate energy measurement of one of the two gamma rays emitted by an individual annihilation, as illustrated in Figure A4 (b). With a Doppler broadened line-shape measurement, the distribution of the annihilation gamma ray energies about the nominal energy of 0.511 MeV is measured. Less deviation from the nominal 0.511 MeV energy value (more gamma rays detected) in a given period of time or very near 0.511 MeV and fewer detected at other energy levels indicates the presence and relative strength of the defect density.

Figure A4. Positron Annihilation Measurement Techniques



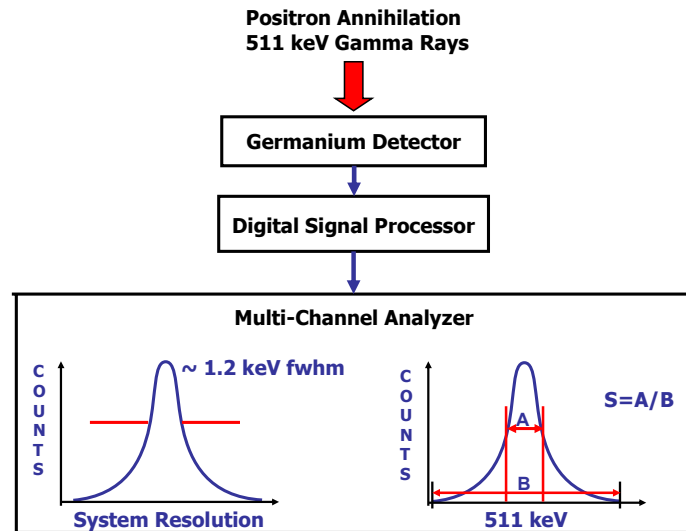
Notes: The three most common experimental positron techniques for measuring electron momentum are (a) angular correlation of annihilation radiation, (b) Doppler broadening, and (c) positron lifetime. When positrons become trapped in defects, there is a reduced overlap with energetic core electrons, leading to less angular deviation (a), more counts at or near the 0.511 MeV peak (b), and longer positron lifetimes (c).

With a positron lifetime measurement, Figure A4(c), the distribution of time between a fiducial gamma ray emitted from the source when the positron is ejected and the annihilation gamma rays observed is measured and provides information not only on the quantity of defects, but due to variations in the lifetime, on the type of defects present.

Although several analytical techniques may be used for positron annihilation analysis, the primary measurement technique to be used in this project is Doppler broadening. This method can provide information not only on the defect concentrations and size, but on the types of defects as well. Figure A5 shows one of the methods used to measure Doppler broadening in this gamma-ray peak.

Doppler broadening effectively compares the relationship of the positron annihilation gammas received in the narrow region surrounding the 511 keV energy level, primarily representing annihilations occurring in the defected areas, against all annihilation energy levels that occur. This “line shaping parameter” or “S” factor for the material is compared to known “S” factors for similar “as manufactured” and failed materials to quantitatively determine defect density and lifecycle percentage.

Figure A5. Doppler Broadening Analysis for the S parameter



Specific elements of the technology that significantly benefit material evaluation are the following:

- Ability to detect bulk properties of materials including: Vacancies and dislocations, GP zones and coherent particles, GP zones associated with occlusions, and incoherent particles.
- Not affected by surface characteristics or component geometry.
- Highly sensitive at low levels of damage or change induced during fabrication, operations, or from induced compressive stress leading to subsurface residual stress.

Quantification of Existing Damage/Life Prediction

The ability of PIPA to quantify lattice structure damage at the atomic level provides information on component/material structural integrity never before available in a field or production environment. This accurate assessment is achieved through an established database of line shaping parameters (“S” factors) for various materials and a known dynamic range of “S” factor values. This dynamic “S” factor range is the difference in “S” factors for “as-manufactured” material compared to failed material. The measured “S” factor during the assessment of a component or material is compared to its position within the dynamic range and an accurate and quantifiable evaluation of existing lattice structure damage is achieved. The operational history of the material or component provides an accurate prediction of remaining life, assuming operational cyclic stresses remain fairly constant. The basic shape of the fatigue/lattice structure damage percent to “S” factor curves for all materials from 0%-100% is consistent and relatively parallel, allowing a rapid and accurate prediction of remaining life with minimal measurements.

LIST OF ACRONYMS

INEEL – Idaho National Engineering and Environmental Laboratory
NDE – Non-Destructive Evaluation
NIPA – Neutron Induced Positron Annihilation
PIPA – Photon Induced Positron Annihilation
SEM – Scanning Electron Microscope